INFORMATION TO USERS

This manuscript has been reproduced from the microfilm master. UMI films the text directly from the original or copy submitted. Thus, some thesis and dissertation copies are in typewriter face, while others may be from any type of computer printer.

The quality of this reproduction is dependent upon the quality of the copy submitted. Broken or indistinct print, colored or poor quality illustrations and photographs, print bleedthrough, substandard margins, and improper alignment can adversely affect reproduction.

In the unlikely event that the author did not send UMI a complete manuscript and there are missing pages, these will be noted. Also, if unauthorized copyright material had to be removed, a note will indicate the deletion.

Oversize materials (e.g., maps, drawings, charts) are reproduced by sectioning the original, beginning at the upper left-hand corner and continuing from left to right in equal sections with small overlaps.

Photographs included in the original manuscript have been reproduced xerographically in this copy. Higher quality 6" x 9" black and white photographic prints are available for any photographs or illustrations appearing in this copy for an additional charge. Contact UMI directly to order.

Bell & Howell Information and Learning
300 North Zeeb Road, Ann Arbor, MI 48106-1346 USA
800-521-0600

CHONDROGENESIS OF THE BRANCHIAL CARTILAGE DURING EMBRYOGENESIS OF THE SEA LAMPREY, *PETROMYZON MARINUS*

A thesis

Submitted to the Graduate Faculty

in Partial Fulfilment of the Requirements

for the Degree of

Masters of Science

in the Department of Anatomy and Physiology

Faculty of Veterinary Medicine

University of Prince Edward Island

Sandra L. Morrison

Charlottetown, P.E.I.

February, 2000

CONDITION OF USE

SIGNATURE PAGES

ii-iii

REMOVED

ABSTRACT

The cartilaginous skeleton of the lamprey, unlike all other vertebrate cartilages, is non-collagenous. Previous studies have shown that there are two distinct types of cartilage present in lamprey characterized by their unique extracellular matrix (ECM) proteins. Most skeletal elements contain lamprin as the major structural protein. However, branchial cartilages contain a second, as yet unnamed non-collagenous protein. The objective of this study was to provide concise temporal and spatial characteristics of branchial chondrogenesis in embryonic lamprey. Morphological and ultrastructural aspects of branchial cartilage chondrogenesis in the embryonic sea lamprey, *Petromyzon marinus*, were examined using light and transmission electron microscopy to determine if this unique cartilage followed similar stages of development as the lamprin-based cartilage and the collagen-based cartilage of all other vertebrates. Branchial cartilage condensations first appeared in the mid-region of the third pharyngeal arch representing the first branchial arch at 13 days post-fertilization (pf). Unlike other vertebrate cartilage condensations, condensing cells in the lamprey branchial arches initially appeared as a one cell wide orderly stack, resembling a stack of coins, with cells closely apposed to each other. This ordered pattern was retained throughout development. Within 24 - 48 hours from the first appearance of this condensation, two new condensations formed, one dorsal and one ventral to the mid-region. By this time, chondrification of the condensation in the mid-region had occurred, evident by extracellular spaces between cells of the mid-region and the presence of extracellular matrix material in these spaces. These three condensations fuse into one branchial arch. Branchial arches 2-7 follow the same pattern of chondrogenesis, with the prechondrogenic mid region of arches 2 and 3 appearing by day 14, arch 4 by day 15, arch 5 by day 16, arch 6 by day 17 and arch 7 by day 20 pf. During the early stages of chondrogenesis (day 13 pf to day 18 pf), growth of the branchial arch condensations appears to be the result of cell recruitment from the surrounding mesenchyme and extracellular matrix secretion. In the later stages (day 19 pf to day 20 pf), cartilage growth appears to be due to cell enlargement and cell proliferation. At 14 days pf, sparse amounts of beaded fibrils representing the ECM protein are seen in the extracellular space. However, immunohistochemical and immunoelectron microscopic procedures did not show a positive reaction to the ECM protein in the first arch until day 16 pf. Staining of the ECM with Weigert's resorcin-fuchsin elastin stain was first observed in the first arch at 17 days pf. Histochemical staining with alcian blue (pH 2.5) which denotes cartilage differentiation showed a positive reaction in the middle of the first four arches at 16 days pf. By 20 days pf, the extracellular matrix surrounding the branchial chondrocytes was arranged in two layers: a subperichondrial layer of mainly collagen fibrils and a territorial layer of ECM protein in the form of beaded fibrils concentrically arranged around the chondrocytes. This study defines the morphogenesis and timing of branchial cartilage chondrogenesis, which are necessary for future studies attempting to determine and correlate the molecular aspects of lamprey cartilage development with morphological events.

ACKNOWLEDGEMENTS

I would like to sincerely thank Dr. Glenda Wright for her guidance, supervision, support and sense of humour throughout this project. I would also like to extend my gratitude to Dr. Sue Dawson and Dr. Chris Lacroix for their continuing help and support.

I would also like to thank Chris Campbell, Debbie LeBlanc, Dorota Wadowska and Danielle Legace for their help in so many things, including the collection and maintenance of lamprey, fixing and processing embryos, sectioning and TEM.

I would like to extend my gratitude to Wayne Petley and Lee Dawson for their help in maintaining the adult lamprey and embryos. Also Glenda Clements-Smith and Michelle Gautier for their roles in preparing artwork and poster presentations. I also gratefully acknowledge Shelly Ebbett, Dave Groman and Tom MacDonald for their assistance in producing light micrographs.

Finally I would like to thank Dr. Glenda Wright for her financial support supplied through an NSERC grant and the Department of Anatomy and Physiology for partial funding of a graduate student stipend.

To my husband Sean for his continual patience and support, and my parents for their optimism and encouragement.

LIST OF FIGURES

LIST OF TABLES

TABLE OF ABBREVIATIONS

arc	Arcualia
b	Blood vessel
BSA	Bovine serum albumin
c	Chondrocyte/ chondroblast
C	Condensation
CNBr	Cyanogen bromide
°C	Degrees Celcius (Centigrade)
DAB	3'3 diaminobenzidine hydrochloride
e	Pharyngeal epithelium
E	Epidermis
eb	Epitrematic bar
ECM	Extracellular matrix
eh	Extrahyal arch
ep	Epitrematic process
g	Gill epithelia
gs	Gill slits
h	Hypotrematic bar
hb	Hypobranchial bar
HRLM	High resolution light microscopy
IX*	Glossopharyngeal nerve
L	Lipid
m	Mesenchyme
mi	Mitochondria
n	Nucleolus
N	Nucleus
nc	Nasal capsule
NC	Notochord
o	Otic capsule
p	Precartilage condensation/ prechondrocyte
P	Pharyngeal space
PBS	Phosphate buffered saline
pc	Prechondrogenic regions
pch	Perichondrium
per	Pericardial cartilage
pf	Post-fertilization
pi	Piston
RER	Rough endoplasmic reticulum
s	Subchordal bar
t	Trabeculae
T	Territorial region
T-Blue	Toluidine blue

TEM	Transmission electron microscopy
X*	Vagus nerve
y	Yolk

TABLE OF CONTENTS

1. INTRODUCTION

1.1 AGNATHANS

According to the fossil record, the first vertebrates were jawless (agnathan). The Agnatha consists of four fossil groups (collectively known as the Ostracoderms) and two extant groups, Myxiniformes (the hagfishes) and Petromyzontiformes (the lampreys) (Forey and Janvier, 1993). Until the 1970's, it was thought that lampreys and hagfishes were closely related. After comparing numerous anatomical and physiological features of lampreys, hagfishes and gnathostomes, Løvtrup (1977) proposed that lampreys were more closely related to gnathostomes than either is to the hagfishes. More recent studies of newly discovered fossils as well as living and previously known fossil agnathans reconfirmed Løvtrup's (1977) view that lampreys are more closely related to the gnathostomes, or "jawed" vertebrates than they are to the hagfishes, indicating that they are the most advanced of the extant agnathans (Forey and Janvier, 1993; Janvier, 1996). The divergence of lampreys from gnathostomes about 500 million years ago (Forey and Janvier, 1993) and their subsequent conservative evolution have made them of considerable interest in evolutionary studies.

1.1.1 Sea Lamprey

Lampreys are eel-like, aquatic vertebrates which spend most of their life in freshwater as a filter-feeding larval form that lies burrowed in the silt substrate of rivers and streams. All lamprey species undergo a metamorphosis to the adult form. During this metamorphosis, extensive changes take place, such as the development of the oral

disc, the appearance of teeth and a rasping tongue, modifications of the gill openings and the enlargement of the fins (Hardisty and Potter, 1971). The sea lamprey, *Petromyzon marinus* is an anadromous parasitic species. The newly metamorphosed adult form migrates to the sea where it lives for 1-3 years, feeding primarily on the blood of teleost fishes, eventually returning to freshwater on their upstream spawning migration. Death follows shortly after spawning.

1.2. LAMPREY EMBRYOLOGY

Piavis (1971), using *P. marinus* reared at 18.4° C, established that there are 18 stages of lamprey embryogenesis from zygote (stage 1) to larva (stage 18) (see Appendix A). Ovulated, unfertilized eggs are telolecithal containing a large amount of yolk with the nucleus at the centre of the animal hemisphere. The fertilization membrane appears immediately after fertilization and is retained up to and including prehatching, stage 13, which occurs 8 to 12 days post fertilization (pf). Cleavage is holoblastic. At the point of hatching, the embryos are already at stage 14 (10-13 days pf) of development. Muscles have started to develop in the head region, enabling the head to undulate and push itself out of the surrounding membrane. At this stage, the heart begins to beat at 40 beats per minute. The gut is yolk-filled and the tail is still curved. Stage 15 is referred to as the pigmentation stage and occurs from 13 to16 days pf. It is the stage where dorsal melanophores appear bilateral to the midbrain. Stage 16, the gill cleft stage (15-17 days pf), is characterized by the appearance of gill clefts, which appear and begin to function in order from the first, most cranially, to the seventh, most caudally. The mouth also

becomes enlarged and hooded by the anterior dorsal lip, and the respiratory rate reaches 120 contractions of the velum per minute.

The final stage of prolarval life is stage 17, known as burrowing (17-33 days pf). This is the stage at which the prolarvae first burrow into the substrate. These animals are between 7.5 to 9 mm in length. The end of this stage is reached when the lumen of the yolk-filled gut opens. Stage 18 is the larval or ammocoete stage. At this point, all systems (with the exception of the reproductive system) are differentiated. The yolk-filled gut is now differentiated into the functional digestive system. The duration of the larval stage varies (anywhere from 3 to 7 years) during which the larvae feed on detritus and grow to at least 12 cm in length, 3 g in weight and have a condition factor (weight in grams/length in $mm^3 \times 10^6$) of at least 1.5 before they enter metamorphosis (Youson, 1997).

1.3. THE VERTEBRATE SKELETON

1.3.1 Gnathostome skeleton

The gnathostome skeleton can be divided into (1) the axial skeleton, which includes the notochord, vertebral column, ribs, sternum, cranium and branchial skeleton , and (2) the appendicular skeleton, consisting of pectoral and pelvic girdles, bones of paired fins and limbs, and skeletal elements of median fins in bony fishes (Kent, 1987).

The skull of vertebrates can be divided into three components; (1) the neurocranium (or chondrocranium) which supports the brain and sense organs, (2) the splanchnocranium (or viscerocranium) which surrounds the oral cavity, pharynx, upper

respiratory tract, and provides support to gills if present, and (3) the dermatocranium which includes the premaxillae, the maxillae, and the nasals (Hildebrand, 1974; Webster and Webster, 1974; Kent, 1987; Carlson, 1988).

1.3.2 The lamprey skeleton

The entire skeleton of the lamprey, except the notochord, is cartilaginous, whereas in all gnathostomes (except the chondrichthyes) it is composed of cartilage and bone (Figure 1.1 A,B).

Lampreys lack an appendicular skeleton, as they have no paired fins or limbs. The axial skeleton of lampreys consists of the notochord, cranium, the branchial basket, the vertebral rudiments or arcualia and dorsal fin rays (Hardisty, 1981). The neurocranium of the ammocoete consists of the nasal and otic capsules, the trabeculae, and the parachordals (Figure 1.1 A). The neurocranium of the adult undergoes very little change during metamorphosis.

The splanchnocranium of the ammocoete has only one structure made of true cartilage, the branchial basket. Mucocartilage, a unique type of connective tissue in the ammocoete splanchnocranium (Wright and Youson, 1982) forms structures such as the prenasal plate (which supports the oral hood), and the walls of the buccal and vestibular cavities. This tissue is more flexible than true cartilage, and is considered to be an adaptation for the burrowing habit and microphagous feeding of the ammocoete (Hardisty and Potter, 1979). Mucocartilaginous tissues change during metamorphosis. Some of these tissues are replaced by muscle, and others by true cartilage (Hardisty,

Figure 1.1

Diagram showing some of the skeletal elements of the A) larval and B) adult sea lamprey. **A.** Cartilaginous structures of the larval sea lamprey include the nasal capsule (nc), trabeculae (t), otic capsule (o), parachordal (para) and the branchial basket, composed of the 7 transverse gill arches. The first arch has a cartilaginous loop, while arches 2-7 each have an epitrematic process (ep). Arches 2-7 are joined dorsally by the subchordal bar (s). All arches are joined in the middle by the hypotrematic bar (h), and ventrally by the hypobranchial bar (hb). Notochord (NC).

B. Cartilaginous structures of the adult sea lamprey include annular cartilage (a), nasal capsule (nc), piston cartilage (pi), trabeculae (t), otic capsule (o), arcualia (arc), pericardial cartilage (per) and the branchial basket. The 7 gill arches are now connected by 4 horizontal bars; the subchordal (s), the epitrematic bar (eb), the hypotrematic (h) and the hypobranchial (hb) bars. An additional structure, the extra-hyal (eh) is present in front of the first branchial arch. Notochord (NC).

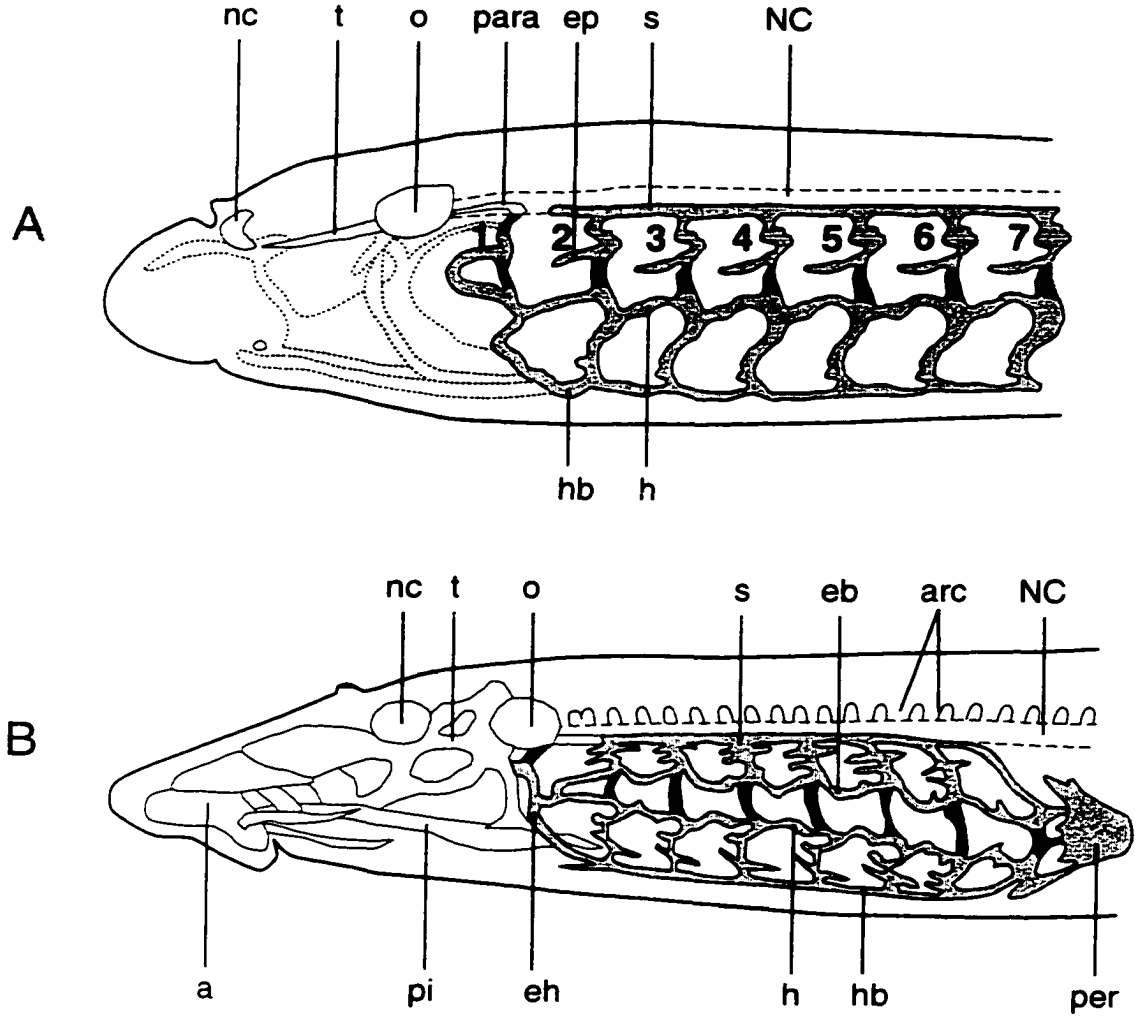
A
nc
t
o
para
ep
s
NC
1
2
3
4
5
6
7
hb
h
B
nc
t
o
s
eb
arc
NC
a
pi
eh
h
hb
per

1979;1981; Armstrong *et al.*, 1987; Janvier, 1993). For example, the mucocartilage of the ventromedial longitudinal bar in the larva differentiates into both muscle and the piston (tongue) cartilage during metamorphosis.

The adult splanchnocranium includes the pericardial, piston, annular (oral disc), and buccal funnel cartilages, as well as the branchial basket (Figure1.1 B).

1.4 THE LAMPREY BRANCHIAL SKELETON

The branchial basket of the ammocoete consists of seven transverse arches that run dorsoventrally, united by a series of three longitudinal rods on each side (Fig1.1 A). These are referred to, according to their position, as the subchordal, hypotrematic and hypobranchial rods or bars (Johnels, 1948; Hardisty, 1981). The subchordal bars are positioned along the ventrolateral surface of the notochord and connect branchial arches 2-7 together. The subchordal bar originates from arch 2 and does not connect to the first arch. The first arch is connected to the caudal end of the parachordal (Johnels, 1948). Each arch has an epitrematic process, which extends cranially in the ammocoete; these processes are connected in the adult to form the epitrematic bar dorsal to the gill clefts (Figure1.1 B). Hypotrematic bars unite adjacent arches ventral to the gill cleft. Unlike the other gill slits in the ammocoete, the first one is completely surrounded by a loop of cartilage. The hypobranchial bars unite adjacent arches in the most ventral position. In the adult, an additional arch, the extra-hyal, is present in front of the first branchial arch. It is joined to the subocular arch dorsally, and ventrally attached to the loop of the first arch and hypobranchial bar (Hardisty, 1981).

1.5 CARTILAGE

1.5.1 Gnathostome cartilages

The majority of information on the developmental, molecular and biochemical characterisation of cartilage comes from studies of avian and mammalian tissues. Unless indicated otherwise, the following descriptions are based on results from these tissues.

There are three types of cartilages distinguished by the type of extracellular matrix present and its components. The extracellular matrix imparts the specific characteristics to a particular cartilage type. Hyaline cartilage is the most common and is characterized by its resilience and ability to withstand compression. It is found on the ventral ends of the ribs, in the tracheal rings, in the larynx and on joint surfaces of bones as articular cartilage. Elastic cartilage is found in the external ear, eustachian tube, laryngeal cartilages, the temporomandibular joint and the sternoclavicular joint, allowing these tissues to undergo expansion and recoil. Fibrocartilage occurs in a few regions where dense connective tissues such as tendons and ligaments merge with hyaline cartilage or bone, such as intervertebral discs and menisci. It is characterized by its tensile strength and resistance to breakage (Mayne and von der Mark, 1983; Fawcett, 1986; Junqueira *et al.*, 1998).

Cartilages are unique in that they are avascular. The nutritional supply to the tissue is achieved by diffusion through the cartilage matrix. Cartilage extracellular matrix is synthesized by chondrocytes (for a review, see Muir, 1995).

1.5.2 Cartilage extracellular matrix

Chondrocytes are mesenchyme-derived. Relative to other tissues, the ratio of cells to matrix in cartilage is low. The cartilaginous matrix is a composite material of fibrous proteins embedded in a proteoglycan aggregate. Collagen type II is the major fibrous collagen found in hyaline cartilage, normally representing 80-90% of the collagen content of the cartilage matrix (Thomas *et al.*, 1994). Elastic cartilage has elastin-containing elastic fibres as a major component of its extracellular matrix in addition to collagen type II (Mecham and Heuser, 1990). Fibrocartilage contains both type I and type II collagens (Mayne and von der Mark, 1983).

Common to all 19 collagen types is the helix structure, in which three left-handed helices (alpha chains) twist around each other to form a superhelix. Each alpha chain contains glycine at every third residue. Proline and hydroxyproline make up about one quarter of the remaining amino acids (Stockwell, 1979).

In addition to collagen type II fibrils, cartilage may also contain collagen types I, III, V, VI, IX, X, XI, and XIII fibrils, depending on the cartilage structure and stage of differentiation (van der Rest and Mayne, 1988; Bruckner and van der Rest, 1994; McBurney, 1995). Collagen types II, IX and XI are considered to be cartilage-specific (Cremer *et al.*, 1998).

Formation of elastic fibres involves the deposition of elastin on a pre-existing supportive scaffold of microfibrils. This glycoprotein scaffold is the first component of the elastic fibre system that can be recognized during the morphogenesis of elastin-containing tissue (Serafini-Fracassini, 1984).

Elastin is one of the most hydrophobic proteins known, and its amino acid composition is unique. One third of the amino acids are glycine, as in collagen, and one ninth are proline. However, unlike collagen, elastin contains very little hydroxyproline and no hydroxylysine. Elastin also contains increased amounts of the non-polar residues valine, leucine, alanine and isoleucine, and very little aspartic acid, glutamic acid, lysine and arginine (Franzblau and Faris, 1981). Two unusual crosslinking amino acids, isodesmosine and desmosine, are also present in elastin. By crosslinking, these lysine-derived residues help contain the elastin molecules in elastic fibres during stretching, and allow them to snap back to their original position (Stockwell, 1979; Franzblau and Faris, 1981).

Elastin is highly insoluble, withstanding solubilization under extreme conditions (eg. 0.1N NaOH at 100°C for 45 minutes). This insolubility is the result of polymerization of elastin monomers through the interchain cross-linking amino acids isodesmosine and desmosine. Because of this insolubility, elastin can be isolated from all other tissues by extraction with hot alkali. Elastin can also be isolated by digesting the tissue in cyanogen bromide (CNBr) to remove all other components. Since elastin does not contain any methionine, it is not digested by CNBr which cleaves proteins at these residues (Franzblau and Faris, 1981). Elastin-containing elastic fibres do not show periodic cross-striations as found in collagen, and tend to form irregular networks between chondrocytes (Stockwell, 1979). Early work on elastin was based on its unique staining properties. Orcein, Weigert's resorcin-fuchsin, and Verhoeff's iron haematoxylin are some of the most widely used stains selective for elastin, although the

basis for the selectivity of these stains is unknown (Mecham, 1993; Pasquali-Ronchetti *et al.*, 1995).

In addition to the cartilage-specific collagens and/or elastin-containing elastic fibres, the extracellular matrix of vertebrate cartilage also contains a proteoglycan aggregate composed of link proteins, hyaluronan and aggrecan (Morgelin *et al.*, 1995).

1.5.3 Lamprey cartilage

Parker (1883) was one of the first to describe the skeleton of the lamprey and defined it as consisting of two types of cartilage, soft and hard. Schaffer (1930) described the cartilage in lamprey as a "true" cartilage, suggesting it was composed of collagen. It was not until 53 years later that the major fibrous component of at least some lamprey cartilages was shown by biochemical (Wright *et al.*, 1983) and ultrastructural (Wright and Youson, 1983) criteria to be composed of a unique non-collagenous protein, which was called lamprin.

Lamprey cartilages show some similarities to elastic cartilage in that they are resistant to digestion by cyanogen bromide (CNBr), are insoluble in boiling 0.1N NaOH, stain with Verhoeff's elastin stain, and have a highly hydrophobic amino acid composition (Wright *et al.*, 1983; Wright and Youson, 1983; Robson *et al.*, 1997).

Lamprin, the major structural protein of the lamprey piston, annular, and neurocranial (trabecular) cartilages has been cloned and characterized (Robson *et al.*, 1993). Lamprin is an insoluble, highly hydrophobic protein with an amino acid content resembling that of elastin, in that proline, glycine, alanine, valine, and leucine make up

over 80% of the entire amino acid content, along with a small amount of acidic amino acids. However, lamprin also contains substantial amounts of tyrosine and histidine, traces of hydroxyproline, and no hydroxylysine, desmosine or isodesmosine (Wright *et al.*, 1983). Ultrastructural studies show that lamprin is present in the matrix of trabecular, annular, and piston cartilages as a dense network of branched fibrils 15-40 nm in diameter which show no cross banded periodicity (Wright and Youson, 1983; Wright *et al.*, 1983; Wright *et al.*, 1988).

Recent studies demonstrate that lamprey branchial and pericardial cartilages differ from lamprin-based trabecular, annular and piston cartilages. *In situ* hybridization studies have indicated the absence of expression of lamprin mRNA in branchial and pericardial cartilages (McBurney *et al.*, 1996a). CNBr- insoluble samples from branchial and pericardial cartilage have an amino acid composition that is different than that of lamprin, containing high amounts of valine, leucine and histidine, and also substantial amounts of hydroxyproline (Robson *et al.*, 1997). In addition, antibodies raised to the CNBr-insoluble residues of branchial cartilage react positively with branchial and pericardial cartilages but not lamprin-based cartilages, while antibodies to lamprin showed a negative reaction to the branchial and pericardial cartilages (Robson *et al.*,1997). These findings show that branchial and pericardial cartilages contain a matrix protein distinctly different than the lamprin of the annular, neurocranial, and piston cartilages.

Verhoeff's staining, insolubility to CNBr and hot alkali treatment, and the amino acid compositions suggest that lamprin and the major matrix protein of lamprey branchial and pericardial cartilage are similar although not identical to insoluble elastin. This is

particularly intriguing since Sage and Gray (1979) after analysing blood vessels in a wide group of vertebrates concluded that elastin-like proteins were not present in agnathans.

1.6 CHONDROGENESIS

1.6.1 Gnathostomes

All components of the skeleton are derived from mesenchyme under the influence of other tissue types. Skeletal components of the limbs, trunk, and parts of the head are of mesodermal origin and those of the face and branchial arch region are of neural crest origin (Carlson, 1988). Neural crest cells originate at the neural tube-ectodermal junction in the early embryo (Langille and Hall, 1993). During embryogenesis, these cells follow extensive migration and differentiation pathways throughout the embryo. The pathway of migration of the crest cells is determined mainly by the influence of the local environment. The neural crest cells forming the neurocranium are influenced by the notochord, whereas those forming the viscerocranium or branchial arches require an inductive influence from pharyngeal endoderm (Carlson, 1988). When the crest cells reach their final destination, they begin to exert an influence over their neighbouring cells, causing them to begin differentiating into different cell types that will form certain structures (Carlson, 1988; Langille and Hall, 1993).

Chondrogenesis can be divided into three major phases: precondensation (characterized by epithelial-mesenchymal interactions), condensation, and differentiation (Hall and Miyake, 1995). Prechondrogenic mesenchymal cells have a small amount of cytoplasm, a few mitochondria, a poorly developed Golgi complex, a sparsely distributed

endoplasmic reticulum with few attached ribosomes (Thorogood and Hinchliffe, 1975; Sheldon, 1983) and may contact each other via elongated filapodia (Thorogood and Hinchcliffe, 1975; Ede, 1983). Intercellular spaces are still easily distinguishable between prechondrogenic cells and no prolonged areas of close apposition of cell surfaces exist (Thorogood and Hinchcliffe, 1975). These cells synthesize type I and III collagens, and non-cartilage type proteoglycans (Sandberg, 1991). The precursor mesenchymal cells then withdraw their cellular processes, becoming rounded in shape, and begin to multiply rapidly, forming a condensation or aggregation of similar cells. Cells in this condensation are in contact with each other via gap junctions (Coelho and Kosher, 1991). They then begin to differentiate and take on characteristic morphological features of chondrocytic cells, such as scalloped borders, large Golgi complexes, many mitochondria, an extensive network of rough endoplasmic reticulum studded with large numbers of ribosomes, and large secretory vacuoles (Thorogood and Hinchliffe, 1975; Ede, 1983; Kosher, 1983; Solursh, 1983; Junqueira *et al.*, 1998). All chondroctyes have glycogen in the cytoplasm and many, particularly in elastic cartilage, have fat droplets (Sheldon, 1983). These changes enable chondrocytes to begin synthesizing the extracellular matrix.

There are many different extracellular matrix and cell surface molecules associated with chondrogenesis. Precondensation is characterized by the growth factors bone morphogenic protein-2 (BMP-2) and transforming growth factor beta (TGFβ), and syndecan-1 and -2, which are cell surface proteoglycan receptors. Versican, a chondroitin sulphate proteoglycan which binds to hyaluronic acid, syndecan-3 (another cell surface proteoglycan receptor), and tenascin, a glycoprotein which binds to chondroitin-sulphate

are up-regulated at the condensation phase. The cell adhesion molecules N-CAM and N-cadherin also appear (Hall and Miyake, 1995). During condensation, a marked increase occurs in mRNAs for type II and type IX collagens and the protein core of cartilage proteoglycan (Sandberg, 1991; Hall and Miyake, 1995). As the precursor cartilage cells differentiate, levels of hyaluronidase and chondroitin sulfate or keratan sulfate in the ECM begin to increase. Hyaluronidase breaks down hyaluronic acid, which is known to block chondrogenesis (Hall and Miyake, 1995). Collagen types II and IX appear and molecules of chondroitin sulphate and/or keratan sulphate join to the core protein to form aggrecan. Many aggrecan molecules bind to a hyaluronic acid molecule, forming aggrecan aggregates (Junqueira *et al.*, 1998; Kiernan, 1990). These aggregates, because of the negative charges on the glycosaminoglycans, bind quantities of water, and in combination with the collagens give the cartilage resilience (Junqueira *et al.*, 1998).

As the extracellular matrix is changing and increasing in density, the chondrocytes become isolated in separate compartments or spaces in the matrix called lacunae, losing contact with other cells and begin to undergo mitosis. As soon as these new daughter cells form, they begin synthesizing new extracellular matrix components (Ede, 1983). The chondrocytes are pushed farther apart as the matrix material increases. This type of cartilage growth is called interstitial growth. The entire cartilage structure is surrounded by a layer of cells called the perichondrium, which merges with the adjacent connective tissue. The cells of this perichondrium have the potential to differentiate into chondrocytes, contributing new cells and matrix to the surface of the mass of cartilage. This type of growth is termed appositional growth (Fawcett, 1986; Carlson, 1988).

1.6.2 Chondrogenesis in lampreys

Much is known about the morphological and molecular characteristics of chondrogenesis in birds and mammals (Hall and Miyake, 1995); yet very little research has been done on this process in lampreys. Classic studies of lamprey skeletal development by Damas (1944) and Johnels (1948) provide excellent information on the overall morphological development of the tissues forming the head skeleton of the lamprey *Lampetra fluviatilis*. However, both of these studies were limited to light microscopic examinations of thick paraffin sectioned material. None of these studies of embryo development used eggs fertilized and raised in controlled laboratory conditions. Johnels' (1948) analysis was confined to only 5 embryonic stages; 317 h (13 days), 355 h (14.8 days), 365 h (15 days), 410 h (17 days) and 618 h (25.75 days) and concentrated on development of the trabeculae of the skull. Damas' (1944) study was more extensive, examining embryonic stages equivalent to Piavis stages 10 to 16 and stage 18, looking at a wide range of developing tissues. Damas (1944) established that the first cartilaginous elements formed are the branchial arches. These arches develop in a cranio-caudal sequence. Lamprey trabecular and branchial arches are derived from the neural crest, suggesting homology between these elements and the trabeculae and visceral arches of gnathostomes which are also neural crest derivatives (Langille and Hall, 1988). Extirpation studies by Langille and Hall (1988) found that the anterior-posterior position of the neural crest cells along the neural rod directly corresponded to the anterior-posterior position of the branchial arches in the lamprey.

Recent studies on the development of the lamprin-based trabecular cartilages

during embryogenesis has defined the temporal and spatial expression of lamprin and the ultrastructural features of the chondrogenic events in the sea lamprey (McBurney, 1995; McBurney and Wright, 1996; McBurney *et al.*, 1996a,b). Mesenchymal condensations first appear by day 17 pf (Piavis stage 17) and have large amounts of intracellular yolk, flattened Golgi saccules, and rough endoplasmic reticulum. By day 18 pf, condensing cells are round in shape. Chondrocyte differentiation occurs by day 19 pf. By day 20 pf, a distinct trabecular cartilage is present with rounded to angular chondrocytes separated by thin seams of extracellular matrix (McBurney and Wright, 1996).

Extracellular matrix in early precondensation stages of the trabeculae (days 15 and 16 pf) is sparse, consisting of scattered groups of banded collagen-like fibrils, 20 nm in diameter. Lamprin mRNA transcripts are first detected at day 19 pf, at the end of the condensation phase (McBurney *et al.*, 1996b) concomitant with the first appearance of lamprin fibrils in the extracellular matrix, unlike type II collagen in collagen-based cartilages of gnathostomes, which begins to be expressed during precondensation (Swalla *et al.*, 1988). The quantity of lamprin transcripts and extracellular matrix material continues to increase throughout cartilage differentiation, as the chondrocytes separate from each other (McBurney and Wright, 1996).

1.7 RESEARCH OBJECTIVES

The research presented in this thesis tests the hypothesis that although branchial cartilage in the lamprey contains a unique extracellular matrix protein, the development of this non-collagen based cartilage will follow stages similar to that known for avian and

mammalian collagen-based cartilage development.

Since branchial cartilages in the lamprey represent another type of non-collagen-based cartilage, it will be important to examine the morphological features of chondrogenesis of this cartilage during embryogenesis for comparison to what is known for the lamprin-based trabecular cartilage, as well as the collagen-based cartilages of higher vertebrates. In order to understand the molecular aspects of cartilage development in embryonic lamprey, the morphological aspects of chondrogenesis must be well characterized. This investigation will provide concise temporal and spatial characteristics of branchial chondrogenesis as well as the morphogenic events involved. Results from this study may also help us in understanding the significance of this unique tissue in regards to the evolution of connective tissue proteins in higher vertebrates.

The research objectives of this study were:

1) To examine the ultrastructural features of branchial cartilage development in the sea lamprey, *Petromyzon marinus*, during embryogenesis. This includes cellular differentiation and temporal distribution of the extracellular matrix components of this cartilage. The ultrastructural features of the developing chondrocytes and the branchial cartilage matrix were examined by transmission electron microscopy (TEM).

2) To investigate the temporal and spatial development of the seven branchial or gill arches and distribution of the unique cartilage matrix protein by routine light microscopy of paraffin sections, high resolution light microscopy of resin sections and TEM. Antibodies against the branchial protein were used in an immunohistochemical

study to define when and where the matrix protein appears.

2. MATERIALS AND METHODS

2.1 PRODUCTION AND MAINTENANCE OF EMBRYOS

Adult sea lampreys were captured during their upstream migration in late May and/or early June 1997 and 1998 at a fish ladder (operated by the Department of Fisheries and Oceans Canada) on the LeHave River in New Germany, Nova Scotia. They were transported to the Fish Health Unit at the Atlantic Veterinary College where they were held in a 1000 litre fibreglass raceway supplied with a continuous flow-through of fresh aerated groundwater (11-15 °C). Lighting conditions alternated between 12 hours of dark and 12 hours of green filtered light as a means of keeping the lampreys subdued. Four to six males and four to six females were placed in separate 200 litre fiberglass tanks supplied with a continous flow through of fresh 18.4 ± 0.5 °C aerated groundwater, where they remained until reaching sexual maturity, which was determined using the external criteria described by Piavis (1961). Sexually mature females develop a swollen, purple ridge caudal to the cloaca and also have a soft, enlarged ventral body wall. Sexually mature males develop a large mid-dorsal ridge and have a white papilla protruding through the cloaca.

Eggs and sperm were extracted manually from unanesthetized sexually mature lamprey. Spermatozoa were collected in 50 ml beakers and stored on ice for a maximum of 30 minutes. Viability of sperm was evaluated by examining motility using a light microscope. Eggs were collected as a monolayer in glass bowls with a diameter of about 8 cm. Several drops of undiluted sperm were applied to the eggs with a Pasteur pipette,

and then mixed throughout the eggs using a clean pipette bulb. The mixture was then covered with aluminum foil and allowed to sit at room temperature for five minutes. Eggs and zygotes were never exposed to light for more than 10 minutes. The mixture was then flooded with fresh 18.4 ± 0.5 °C groundwater, covered, and left at room temperature for 1 hour. The water was then siphoned off the eggs, replaced with fresh water of the same temperature and then bowls were placed in an 18.4°C incubator. Water was changed at 4 hours post-fertilization (pf), and then at 12 hour intervals, always at an incubator temperature of 18.4°C. After 24 hours, eggs were examined under a dissecting microscope to remove dead or unfertilized eggs and contaminating material from the embryo culture. Healthy embryos at this stage appeared evenly taupish-colored and round. From 10 days pf, embryos were staged using criteria of external appearance set out by Piavis (1971, Appendix A). Post-gastrulation embryos (days 4-5 pf) were placed in modified Heath trays with continuously running 18.4 ± 0.5 °C groundwater.

2.2 LIGHT MICROSCOPY

Ten embryos were collected daily beginning on day 11 pf (Piavis stage 14: hatching) through to and including day 33 pf (Piavis stage 18: larval). All embryos were anesthesized in 0.05% tricaine methanesulfonate (MS-222) prior to fixation. The embryos were then fixed *in toto* for 24 hours in Bouin's fixative, dehydrated through an ascending series of ethanols, cleared in xylene and embedded in paraffin (Appendix B). Five to 6 μm thick serial transverse sections were cut using a Spencer "820" rotary microtome and mounted on glass slides which had been previously coated with a 2% silane-acetone

solution. Tissue was stained with (1) alcian blue, pH 2.5 which stains sulphated and carboxylated proteoglycans and counterstained with nuclear fast red (Kernechtrot) (Humason, 1972) and (2) Weigert's resorcinol-fuchsin elastic stain (Montes, 1992).

Four to six embryos each of ages 12.5 days pf (Piavis stage 14: hatching) to 20 days pf (Piavis stage 17: burrowing) and larval day 39 pf (Piavis stage 18: larval) were fixed in glutaraldehyde and osmium tetroxide, processed and embedded in Epon/Araldite (see section 2.4 for details). Sequential lateral or horizontal 1 μm thick resin sections were cut through the branchial region using a Reichert Jung Ultracut E microtome(Leica Canada, Halifax, Nova Scotia). Sections were then placed on clean glass slides, and stained with toluidine blue (1% in 1% sodium borate solution) for high resolution light microscopical (HRLM) analysis. All sections stained for HRLM were photographed with a Zeiss Photoscope III (Carl Zeiss Ltd., Ontario).

2.3 LIGHT MICROSCOPIC IMMUNOHISTOCHEMISTRY

Three to four Bouin's-fixed embryos (see Section 2.2 for details) of each age from 15 days pf to 19 days pf were used for immunohistochemical analysis. Five to 6 μm thick serial transverse sections were cut on a rotary microtome and mounted on clean glass slides (5-6 sections/slide). Tissue was then deparaffinized in xylene, rehydrated through a graded series of ethanol to water, then placed in 0.1M phosphate-buffered saline (PBS) pH 7.6 for 20 minutes at room temperature. Phosphate-buffered saline was then replaced by a 30% normal goat serum (Cedarlane Laboratories, Hornby, Ontario) diluted in PBS for 40 minutes at room temperature. Normal goat serum was drained off the sections and

replaced with rabbit antibodies to CNBr insoluble lamprey branchial cartilage (Robson *et al.*, 1997) diluted 1:1000, 1:800, and 1:200 in PBS. Tissue was left to incubate with the antibodies in a moisture chamber at 4°C for 48 hours. After incubation, tissue was rinsed in PBS, and then allowed to sit in PBS for 20 minutes at room temperature. Goat anti-rabbit IgG (Cedarlane Laboratories) diluted 1:10 in PBS was applied and left on the tissue for 1 hour at room temperature. Sections were then rinsed with PBS and left in PBS for 20 minutes. Rabbit peroxidase anti-peroxidase (Cedarlane Laboratories, Hornby, Ontario) was applied to the tissue, diluted 1:25 with PBS, and left for 1 hour. Tissue was rinsed with PBS and washed in 0.05M Tris-HCl buffer, pH 7.6-8.0 for 20 minutes. Sections were then incubated in fresh 0.05% 3,3'-diaminobenzidine hydrochloride (DAB) containing 0.02% hydrogen peroxide in 0.05M Tris-HCl buffer pH 7.6 for 20 minutes. Tissue was rinsed with Tris-HCl buffer and dehydrated through a series of graded ethanols, cleared in xylene and coverslipped. Immunoreactivity was visualized by the formation of a brown insoluble precipitate over antigenic sites. Older animals containing differentiated cartilage were used as positive controls (24 day pf and 39 days pf). Negative controls consisted of replacing the primary antibodies with PBS. Previous investigation has demonstrated the specificity of the primary antibodies to lamprey branchial cartilage and that the antibodies do not cross-react with rat ear cartilage (elastic cartilage) when tested by similar immunostaining (Robson *et al.*, 1997).

2.4 TRANSMISSION ELECTRON MICROSCOPY

For electron microscopic examination, four to six embryos were collected daily

from day 12 pf (Piavis stage 14: hatching) through to and including day 20 pf (Piavis stage 17: burrowing), and on day 39 pf (Piavis stage 18: larval). Embryos were anesthesized in 0.05% MS-222 and fixed *in toto* for two hours at 4 °C in 2.5% glutaraldehyde in 0.1 M Sorenson's phosphate buffer pH 7.3 (Dykstra, 1993). The animals were then rinsed in buffer and post-fixed for one hour at room temperature in similarly buffered 1% osmium tetroxide. Samples were rinsed in buffer, dehydrated through a series of graded ethanols and embedded in a mixture of Epon/Araldite via propylene oxide (Appendix C).

Sections 0.55μm thick were cut using a Reichert Jung Ultracut E ultramicrotome and heat-fixed (dried at 65 °C) to clean glass slides and stained with 1% toluidine blue in a 1% sodium borate aqueous solution. These were used to localize the developing cartilage, and also to judge quality of tissue preparation under light microscope. Ultrathin sections of 85 to 100 nm thickness (gold to silver interference color) were cut in a horizontal and lateral plane through the branchial region using the ultramicrotome, and collected on JBS EM 200 copper grids (JB EM, Dorval, Quebec). These sections of tissue were stained for 30 minutes with saturated uranyl acetate in 50% ethanol, washed with distilled water using a dropper for 1 minute, then stained with Sato's lead stain (Sato, 1968) for two minutes. Stained sections were examined and photographed using a Hitachi H-600 electron microscope (Nissei Sangyo Canada Inc., Rexdale Ontario) operated at 75 kV.

2.5 IMMUNOELECTRON MICROSCOPY

For immunoelectron microscopic examination, four to six embryos were collected daily on day 13 pf (Piavis stage 14: hatching) through to and including day 20 pf (Piavis stage 17: burrowing) and day 39 pf (Piavis stage 18: larval). Embryos were euthanized and fixed *in toto* in 2.5% glutaraldehyde in 0.1 M Sorenson's phosphate buffer pH 7.3 and post-fixed for one hour at room temperature in similarly buffered 1% osmium tetroxide (see section 2.4 for details) or in 2.5% gluteraldehyde in 0.1M Sorensen's phosphate buffer pH 7.3 without post fixation in osmium tetroxide. Samples were rinsed in buffer, dehydrated through a series of graded ethanols and embedded in a mixture of Epon/Araldite via propylene oxide (Appendix C).

Ultrathin sections of 85 to 100 nm thickness (gold to silver interference color) were cut horizontally and laterally through the branchial region on a Reichert Jung Ultracut E ultramicrotome, and collected on nickel grids (Super200, Marivac, Halifax, Nova Scotia). The drop method was used for incubating the grids. When washing, care was taken to only wet the side of the grid containing the tissue. Grids were placed on drops of 0.5M glycine in PBS at room temperature for 30 minutes, rinsed with PBS from a dropper for about 2 minutes and then placed on drops of 1% bovine serum albumin (BSA) in PBS for 10 minutes at room temperature. Grids were then incubated overnight at 4°C in a moisture chamber on drops of rabbit antibodies to CNBr insoluble lamprey branchial cartilage diluted 1:100 or 1:50 in 1% BSA. Grids were washed with 1% BSA for about 2 minutes and then incubated for 30 minutes at room temperature on drops of protein A gold (20nm diameter, Ted Pella Inc., Redding, California) diluted 1:50 in PBS.

Grids were then washed with PBS for about 2 minutes and then with distilled water for 2 minutes.

After the final washing, grids containing the tissue were stained for 30 minutes with saturated uranyl acetate in 50% ethanol, washed with distilled water, then stained with Sato's lead stain for two minutes. Grids were then examined and photographed using a Hitachi H - 600 transmission electron microscope (Nissei Sangyo Canada Inc., Rexdale, Ontario) operated at 75 kV.

2.6 3-D IMAGING

Lateral serial resin sections 1 μm thick stained with 1% toluidine blue were used for 3-D imaging. Two to three embryos from each of day12.5 pf (Piavis stage 14:hatching) to day 20 pf (Piavis stage 17: burrowing) were examined and sequential images were then captured using a digital camera (Panasonic Wv-bp500, Carsen group Inc., Toronto). These digital images were converted into bitmap images using Matrox Inspector Version 1.7 (Matrox Electronic Systems Ltd., Dorval, Quebec). The bitmaps were entered into Surfdriver (Department of Anatomy and Reproductive Biology, University of Hawaii, 1997), a 3-D imaging program. Each piece of developing cartilage on every sixth bitmap was outlined, and the outlines lined up to form a 3-D image of the branchial basket for each age.

2.7 STATISTICAL ANALYSIS

Statistical analysis was carried out using Minitab for Windows (Minitab Inc.

1994, State College, Pennsylvania). Three to four animals of each age, from 13 to 20 days pf were used for each statistical value. Cells in the middle region of the developing first branchial arch of each age were measured using a light microscope ocular scale along their length, perpendicular to the long axis of the branchial bar, to obtain the mean diameter of the cells (n=20) in lateral resin sections. Cells in the same area of the first arch of days 15-17, 19 and 20 pf were also measured to obtain an average thickness of the cells in this area (n=20). For both sets of values, unpaired Student *t*-tests were carried out to determine if the arch increased in diameter with age, and if the chondrocytes increased in thickness. Analysis of variance (ANOVA) was performed on means of cell thickness from 15 to 39 days pf and cell widths from 13 to 39 days pf to determine if there was a significant increase in these parameters during development. P-values greater than 0.05 were considered insignificant.

2.8 CHEMICALS AND REAGENTS

Chemicals and reagents used throughout this project were supplied by: Sigma, St. Louis, Missouri (MS-222, alcian blue, Tris-HCl buffer reagents, hydrogen peroxide, toluidine blue, sodium borate), Fisher, Fairlawn, New Jersey (histological grade xylene, Paraplast, reagents for Weigert's resorcin-fuchsin), Canemco, St. Laurent, Quebec (EM grade glutaraldehyde, Epon/Araldite, osmium tetroxide) and Marivac, Halifax, Nova Scotia (lead acetate, citrate). Ethanol was supplied by Commercial Alcohols Inc., Brampton, Ontario and 3,3'-diaminobenzidine hydrochloride was purchased from Polysciences Inc., Warrington, Pennsylvania.

3. RESULTS

3.1 HIGH RESOLUTION LIGHT MICROSCOPY

Using HRLM, it was found that the development of branchial cartilages (henceforth referred to as branchial arches) within each of pharyngeal arches 3 to 9 followed the same pattern. The differentiation of the gill cartilages appeared first as a small bar-shaped condensation in the middle of the mesenchyme in each pharyngeal arch except the first and second, with the dorsal and ventral portions of the condensation developing subsequently, resulting in the elongation of the arches both dorsally and ventrally at the same time.

Analysis of lateral (sagittal) sections through the developing pharyngeal arches demonstrated that the first branchial arch can be identified consistently in all 13 day post-fertilization embryos examined within the third pharyngeal arch. The presence of bar or rod-shaped precartilage (or prechondrogenic) condensations representing branchial arches 2 and 3 was variable at 13 days pf (Figure 3.1.1 A). Prechondrogenic cells were distinguished from surrounding mesenchyme by their arrangement in a tightly packed condensation which was rod-shaped and oriented such that the long axis was dorsoventrally aligned. The precartilage condensations were oriented caudal to and parallel with the cranial nerves which innervate the pharyngeal arches (Figure 3.1.2). The prechondrogenic condensation of the first, second and third branchial arches, viewed in a sagittal plane, consisted of elongated wedge-shaped cells stacked one upon another in an irregular fashion with the long axis of each cell more or less perpendicular to the dorsoventral axis of the pharyngeal arch. Cells were closely apposed to each other with

Figure 3.1.1
3-D reconstruction of developing branchial arches of embryonic sea lamprey. Arches are in cranio-caudal order from left to right. All reconstructions are lateral views of one set of branchial arches on the left side of the animal looking from the outside into the pharynx. **A)** 13 days pf : arches 1-3, Bar = 57 μm **B)** 14 days pf : arches 1-4, Bar = 52 μm **C)** 15 days : arches 1-4, Bar = 53 μm **D)** 16 days pf : arches 1-5, with arches 1-4 beginning to curve. Bar = 61 μm

A

B

C

D

Figure 3.1.2
One μm thick sagittal section through the first branchial arch condensation of a 13 day pf embryo. The precartilage condensation (p) is aligned parallel and caudal to the glossopharyngeal nerve (IX*). There is very little extracellular space (arrow) between prechondrocytes. Note the large lipid droplets (arrowhead) in some of the cells. Mesenchyme (m), pharyngeal space (P), pharyngeal epithelium (e), yolk (y).
Bar = 10 μm


P

very little extracellular space between them (Figure 3.1.2). The average diameter (± standard deviation) of the cells forming the first bar was 17.1 ±1.8 μm (n=20).

By 14 days pf, condensations representing branchial arches 1, 2 and 3 were consistently present (Figure 3.1.1 B). Cells of these condensations appeared similar in shape to those of 13 days pf, but those of arches 1 and 2 were less tightly packed with more obvious extracellular spaces between cells (Figure 3.1.3). These cells were now termed prechondrocytes or chondroblasts, a term used to describe cells in the transition from prechondrogenic mesenchymal cells to chondrocytes. The average diameter of the chondroblasts forming the first branchial arch condensation was 15.6 ±1.2 μm (n=20), which was statistically different than those at 13 days pf ($p = 0.004$). Cells appeared circular in horizontal sections (Figure 3.1.4).

By 15 days pf, branchial arches 1-4 were present (Figure 3.1.1). Arches 1 and 2 appeared similar, with lateral profiles that consisted of regularly aligned elongated rectangular to wedge-shaped cells partially separated from each other by distinct narrow extracellular spaces (Figure 3.1.5). Based on the distinct separations between cells, the first two branchial arches can now be considered chondrogenic or cartilaginous. At this point in development, the chondrocytes were stacked in a more regular aligned fashion. Chondrocytes of the first arch had an average thickness of 1.7 ± 0.5 μm (n=20). The average diameter of the cells in the first arch was 16.0 ±1.3 μm (n=20) which was not statistically different than those at 14 days pf ($p=0.32$). Two new precartilaginous condensations appeared extending dorsally and ventrally from the middle origin, the now cartilaginous first arch. These dorsal and ventral regions consisted of wedge-shaped cells

Figure 3.1.3
Sagittal section through the first branchial arch condensation of a 14 day pf embryo. Narrow, incomplete extracellular spaces are seen between and surrounding cells (arrow) of the condensation. Pharyngeal space (P), pharyngeal epithelium (e), glossopharyngeal nerve (IX*), yolk (y). Bar = 13 μm

Figure 3.1.4
Horizontal section through the pharyngeal wall of a 14 day pf lamprey shows that the first branchial arch condensation (C) in transverse section is only one cell wide. Lipid (arrowhead), pharyngeal epithelium (e), pharyngeal space (P), glossopharyngeal nerve (IX*). Bar = 11 μm


P
P
P
IX

Figure 3.1.5
Sagittal section through the mid-ventral region of the first branchial arch of a 15 day pf embryo. Chondrocytes are elongated and stacked upon each other, separated by a well-defined extracellular space (arrow). The ventral region of this arch (outlined by a dotted line) is prechondrogenic, with cells closely packed, exhibiting very little extracellular space. Glossopharyngeal nerve (IX*), pharyngeal space (P). Bar = 13 μm

Figure 3.1.6
Sagittal section through the prechondrogenic condensation (outlined by a dotted line) of the fourth branchial arch of a 15 day pf embryo. Note the irregularly aligned stack of wedge-shaped prechondrocytes (p) and incomplete extracellular spaces (arrow) compared to the cartilaginous portion of the first arch in Figure 3.1.5. Pharyngeal space (P), vagus nerve (X*). Bar = 10 μm

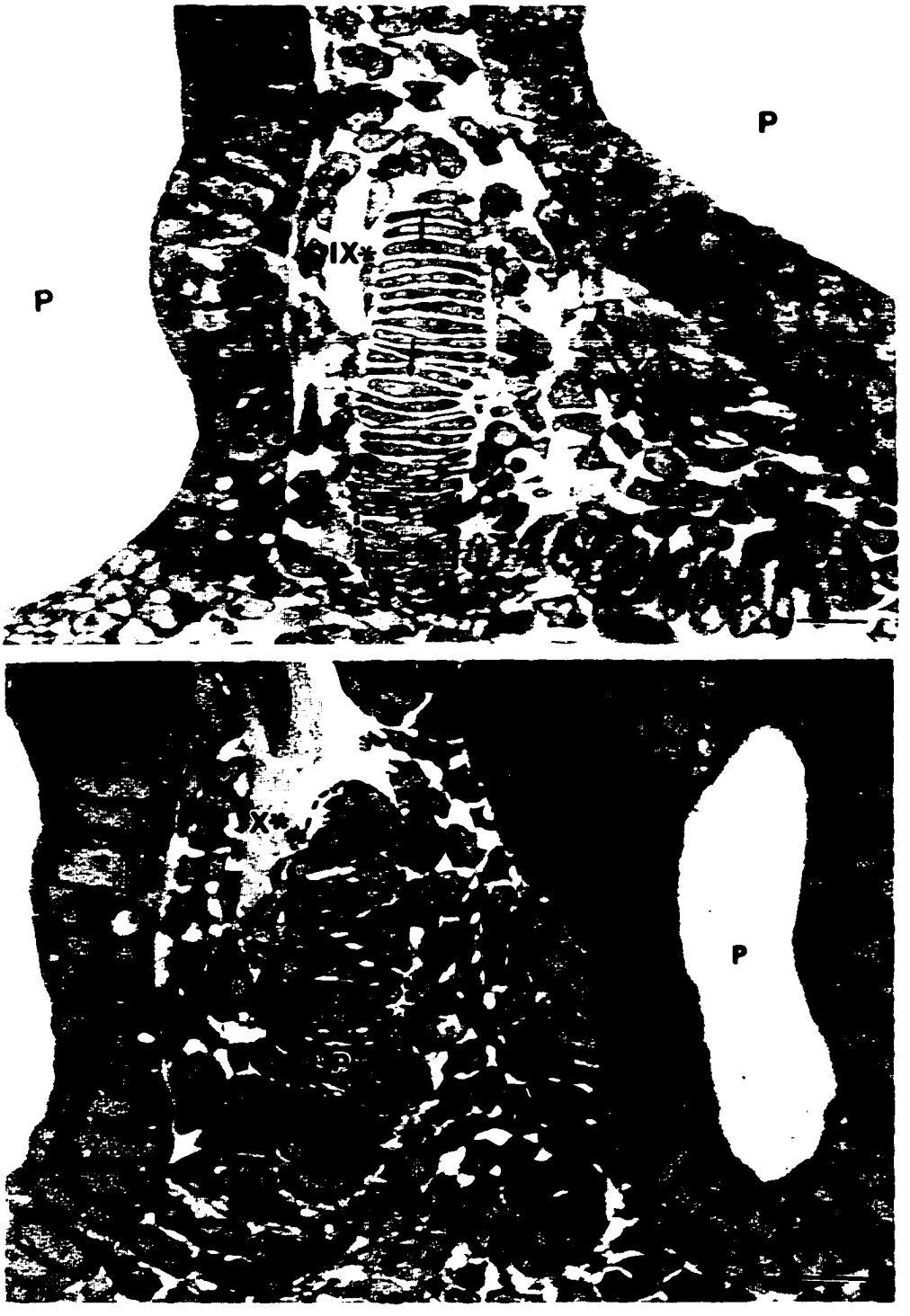
P
P
IX*
X*
P

that were more tightly packed than the chondrocytes in the middle region of the arch (Figure 3.1.5). At this specific age of embryogenesis, condensations of the third and fourth branchial arches were prechondrogenic, consisting of cells that were irregularly aligned in a dorsoventral stack and partially separated by extracellular spaces (Figure 3.1.6).

Five branchial arches were present by 16 days pf and arches 1-3 were all curved medially (Figure 3.1.1 D). The mid region of arches 1-4 were now cartilaginous, consisting of chondrocytes separated by distinct extracellular spaces (Figure 3.1.7). Most chondrocytes were elongated, spindle to rectangular-shaped cells, uniformly arranged like rungs on a ladder, although a few triangular shaped chondrocytes wedged between neighboring cells disrupted this arrangement (Figure 3.1.7). The average diameter of the chondrocytes in the mid region of the first bar increased significantly to18.5 ± 1.3 μm (n=20, $p < 0.001$) compared to cells at earlier stages of development. Chondrocytes were circular shaped in horizontal sections through the middle region of the first arch (Figure 3.1.8). Chondrocytes in the middle region of the first arch had an average thickness of 2.2 ± 0.4 μm (n=20), which was significantly different than that of 15 days pf cells ($p= 0.001$). A perichondrium was now visible around the middle chondrogenic region of the first 4 arches, consisting of a single layer of rounded to cuboidal shaped cells separating the peripheral extracellular region of the newly formed cartilage from the rest of the cells forming the pharyngeal arch (Figure 3.1.7) Dorsal and ventral extensions of the first arch were also chondrogenic, while those of the second, third and fourth were prechondrogenic (Figure 3.1.9). The middle region of the fifth arch was prechondrogenic,

Figure 3.1.7
Sagittal section through the mid region of the first (left) and second (right) branchial arches of a 16 day pf embryo. Chondrocytes are separated by distinct extracellular spaces, and the perichondrium is beginning to form around the arches (arrow). Intercalated cells (arrowhead) can be seen wedged between chondrocytes. Glossopharyngeal nerve (IX*), vagus nerve (X*), pharyngeal space (P). Bar = 16 μm

Figure 3.1.8
Horizontal section through the pharyngeal wall of a 16 day pf embryo. The first branchial arch in transverse section consists of a large circular chondrocyte (c) with an eccentric bean-shaped nucleus (N). Perichondrium (arrow), pharyngeal space (P). Bar = 10 μm

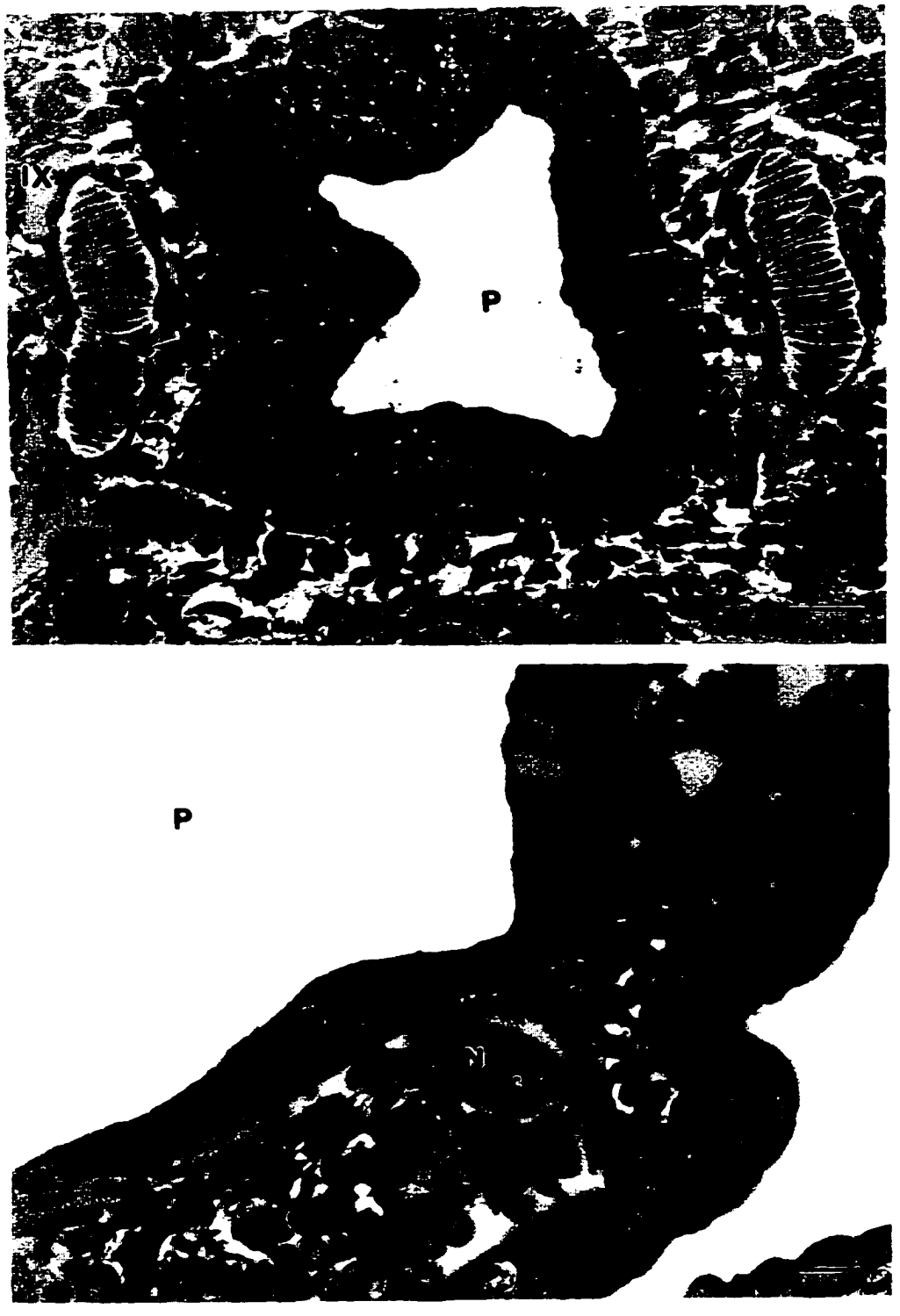
IX
P
P

Figure 3.1.9
Sagittal section through the mid-dorsal region of the third branchial arch of a 16 day pf embryo. Dorsal region of arch is prechondrogenic (outlined by a dotted line) with wedge-shaped cells, while the mid region is chondrogenic with elongate chondrocytes separated by distinct extracellular spaces (arrow). Perichondrium (pch), pharyngeal space (P). Bar = 10 μm

Figure 3.1.10
Sagittal section through the mid-dorsal region of the fifth branchial arch of a 16 day pf embryo. Wedge-shaped prechondrocytes (p) with incomplete extracellular spaces between the cells (arrowhead) form the mid region. The dorsal region is made up of condensing prechondrogenic or precartilaginous cells (outlined by a dotted line). Pharyngeal space (P), vagus nerve (X*). Bar = 8 μm

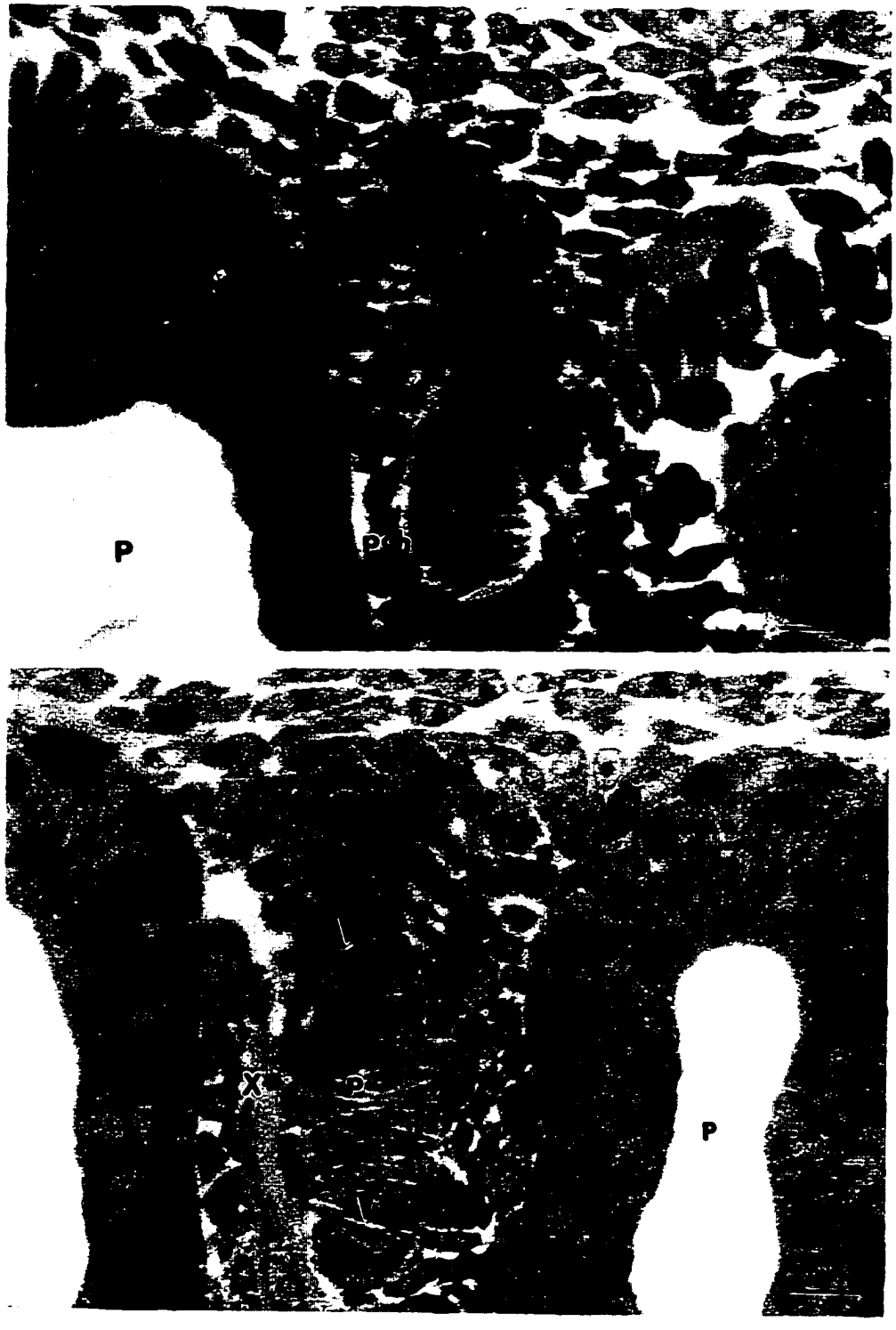
P
P
X
P

with the dorsal and ventral regions consisting of newly condensing precartilage cells (Figure 3.1.10).

At 17 days pf, there were 6 branchial arches present (Figure 3.1.11 A). Arches 1-5 were cartilaginous, with distinct extracellular spaces separating and surrounding the chondrocytes and a peripheral single cell layer of perichondrial cells (Figure 3.1.12). The average diameter of chondrocytes in the middle region of the first arch at 18.4 ± 1.2 μm (n=20) was not significantly different than those at 16 days pf (p=0.8). The average thickness of chondrocytes in the middle region of the first arch at this stage was 2.3 ± 0.6 μm (n=20), which was not significantly different than that of 16 days pf (p=0.75). Chondrocytes were circular in shape in horizontal sections through the middle region of the first arch (Figure 3.1.13). The sixth arch consisted of wedge-shaped prechondrocyte cells partially separated by extracellular space (Figure 3.1.14).

Six branchial arches were present at 18 days pf. The first arch had developed two rod-shaped condensations that projected anteriorly, dorsal and ventral to the middle region (Figure 3.1.11). Chondrocytes in the middle regions of arches 1 and 2 appeared different than those of 3, 4 and 5 (Compare Figure 3.1.15 and Figure 3.1.16). Boundaries between cells in arches 1 and 2 were indistinct and extracellular spaces between cells were difficult to resolve. Because of this, the average thickness of the chondrocytes in arches 1 and 2 could not be determined at this stage, although chondrocytes appeared thicker than those at 17 days pf. Chondrocytes in the middle region of the first arch were not significantly different (p=0.81) in diameter than those at 17 days pf, with an diameter of 18.3 ±1.3 μm (n=20) and were circular in shape in horizontal sections (Figure 3.1.17).

Figure 3.1.11
3-D reconstruction of developing branchial arches of embryonic sea lamprey. Arches are in cranio-caudal order from left to right. **A-C)** reconstructions are lateral views of one set of branchial arches on the left side of the animal, looking from the outside in to the pharynx. **D)** is a reconstruction of the right side of the embryo, the medial view looking from the pharynx to the outside.
A) 17 days pf Arches 1-6; Two different shades were used to provide an example of the boundaries between chondrogenic and prechondrogenic regions. The mid regions are chondrogenic (dark grey) and dorsal and ventral regions are prechondrogenic (light grey). The sixth arch is entirely prechondrogenic. Bar = 62 μm **B)** 18 days pf Arches 1-6, both chondrogenic and prechondrogenic regions are dark grey. Bar = 92 μm **C)** 19 days pf Arches 1-6, showing greater curvature in dorsal and ventral regions than 18 days pf. Bar = 97 μm **D)** 20 days pf Arches 1-7. Arches are connected by the ventral hypobranchial bar, and possess dorsal and mid projections. The first arch now has a cartilaginous loop that surrounds the first gill opening. Bar = 104 μm

A

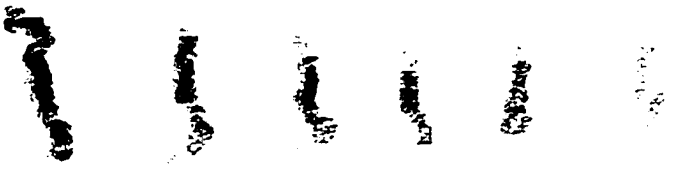

B

C

D

Figure 3.1.12
Sagittal section through the mid-dorsal region of the second branchial arch of a 17 day pf embryonic lamprey. Chondrocytes (c) in the mid region are rectangular-shaped, and separated by wide extracellular space (arrow) compared to cells in the dorsal region which are wedge-shaped and closer together. A single-cell layer perichondrium (arrowhead) surrounds the mid region of the arch. Pharyngeal space (P), vagus nerve (X*). Bar = 10 μm


P

Figure 3.1.13
Horizontal section through the pharyngeal wall of a 17 day pf lamprey. The mid region of the fourth branchial arch appears in transverse section as one large oval shaped chondrocyte (c) with an eccentric nucleus (N) and surrounded by a wide extracellular space (arrow) and a perichondrium (arrowhead). Pharyngeal space (P), gill slit (gs). Bar = 10 μm

Figure 3.1.14
Sagittal section through the mid region of the prechondrogenic condensation forming the sixth branchial arch of a 17 day pf embryonic lamprey. Pharyngeal space (P), vagus nerve (X*), mitotic figure within branchial condensation (open arrow). Bar = 8 μm

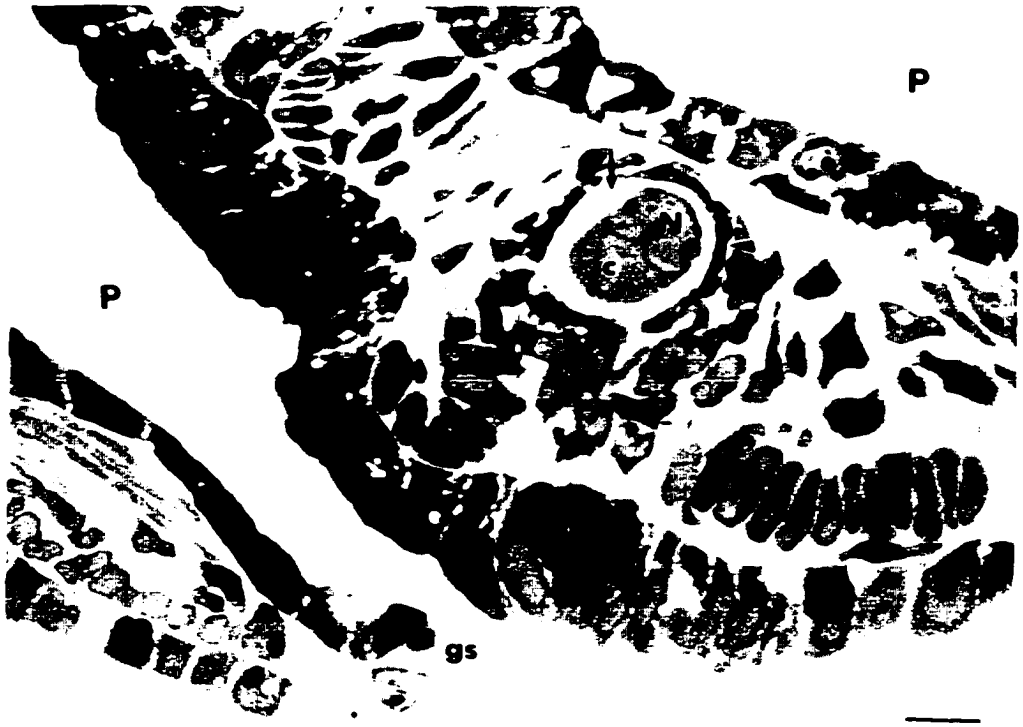
P
P
gs

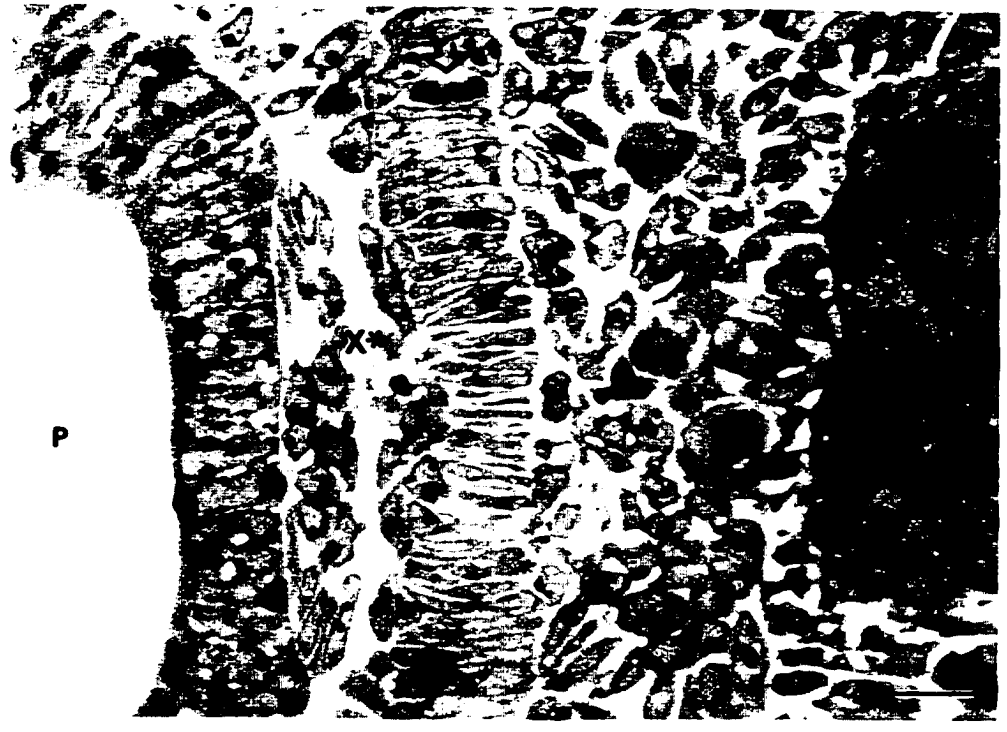
X
P

Figure 3.1.15
Sagittal section through the mid-ventral region of the second branchial arch of an 18 day pf embryo. Boundaries between chondrocytes (c) are indistinct (arrowhead) but chondrocytes appear thicker than in the same arch at 17 days pf (compare with Figure 3.1.12). Pharyngeal space (P). Bar = 13 μm

Figure 3.1.16
Sagittal section through the mid-ventral region of the fourth branchial arch of an 18 day pf embryo. Note the rectangular-shaped chondrocytes in the mid-region separated by distinct extracellular spaces (arrowhead). Prechondrocytes (p) in the ventral region are wedge-shaped and stacked closer together. Pharyngeal space (P), vagus nerve (X*), perichondrium (pch).
Bar = 9 μm


P
P
P
P
pch

Figure 3.1.17
Horizontal section through the pharyngeal wall of an 18 day pf lamprey, showing that the mid region of the first branchial arch is still only one cell wide. Chondrocyte (c), eccentric nucleus (N), perichondrium (arrow), gill slit (gs), pharyngeal space (P).
Bar = 10 μm

Figure 3.1.18
Sagittal section through the mid-dorsal region of the sixth branchial arch of an 18 day pf embryo showing chondrocytes in the mid-region separated by distinct extracellular spaces (arrowhead) and prechondrogenic cells (outlined by a dotted line) in the dorsal region. Pharyngeal space (P), vagus nerve (X*), perichondrium (pch). Bar = 10 μm


P
P
N
C
gs
P

The sixth arch at this stage was cartilaginous, with chondrocytes in the middle of the arch separated by distinct extracellular spaces, similar in appearance to those in arches 3, 4 and 5 (Figure 3.1.18). Mitotic figures were occasionally seen in arches 1-5 in days 17 and 18 pf (Figure 3.1.14).

At 19 days pf, six branchial arches were present and all were cartilaginous. Reconstruction from serial sections reveals that arches 1-4 were S-shaped dorsally and ventrally (Figure 3.1.11). The diameter of the chondrocytes in the middle region of the first arch was 19.4 ± 1.6 μm (n=20), which was significantly different (p=0.024) than that of 18 days pf cells. Toluidine blue staining revealed an extracellular matrix surrounding and separating the chondrocytes in arches 1 and 2 (Figure 3.1.19). Chondrocytes in these arches appeared thick and rectangular to disc-shaped, with an average thickness of 3.5 ± 0.6 μm (n=20), which was significantly different than that of 17 days pf cells ($p < 0.001$). Arches 3, 4 and 5 have chondrocytes with indistinct boundaries between cells. Chondrocytes in arch 6 were separated by distinct extracellular spaces. Mitotic figures were prevalent in arches 1-4 (Figure 3.1.19).

By 20 days pf, all seven branchial arches were present. The anterior condensations from the middle region of the first arch have fused to form a cartilaginous loop surrounding the first gill opening (Figure 3.1.11). The subchordal and hypotrematic bars that connect arches 2-6 were not completely formed at 20 days post-fertilization. Arches 2 through 6 have all developed two anterior projections, representing the epitrematic processes dorsally and the beginning of the formation of the hypotrematic bar ventrally. Arches 1-6 were connected ventrally by the developing hypobranchial bar (Figure 3.1.11).

Figure 3.1.19
Sagittal section through the mid-dorsal region of the first branchial arch of a 19 day pf embryo. Extracellular matrix surrounding the chondrocytes stains with toluidine blue (arrow). Mitotic figures are prevalent at this stage (arrowhead). Glossopharyngeal nerve (IX*), pharyngeal space (P).
Bar = 13 μm

Figure 3.1.20
Sagittal section through the mid region of the first branchial arch of a 20 day pf embryo. The arch is now 1-2 cells wide. Chondrocytes (c) are surrounded by a toluidine-blue staining extracellular matrix (arrow). Blood vessel (b), gill epithelia (g). Bar = 13 μm

Figure 3.1.21
Horizontal section through the pharyngeal wall of a 20 day pf lamprey, showing that in transverse section the first branchial arch is circular shaped and two cells wide. Chondrocyte (c), nucleus (N), perichondrium (pch). Bar = 10 μm


P
b

The middle region of the first arch was now 1-2 cells wide (Figures 3.1.20 and 3.1.21) with an average diameter of 20.8 ± 1.2 μm (n=20), which was significantly different than that at 19 days pf ($p = 0.004$). Chondrocytes in the middle region of the first arch had an average thickness of 4.7 ± 1.0 (n=20), which was significantly different than that at 19 days pf ($p < 0.001$). The extracellular matrix material between and around chondrocytes of branchial arches 1-4 stained with toluidine blue, revealing the outline of the chondrocytes (Figures 3.1.20 and 3.1.22), however in arches 5 and 6, cell boundaries were hard to define, and spaces between cells were difficult to resolve (Figure 3.1.23). The seventh arch was consistently present with a chondrogenic mid region of regularly stacked cells separated by extracellular space and surrounded by a perichondrium and dorsal and ventral prechondrogenic regions (Figure 3.1.24).

In lateral sections of a 39 day pf larval lamprey, all arches were at least 2 cells wide. Chondrocytes in the middle region of the first arch had an average thickness of 7.4 ± 1.0 μm (n=20), which was significantly different than that of 20 days pf ($p < 0.001$). Chondrocytes varied in shape, appearing rounded, rectangular, or cuboidal with pale-staining cytoplasm. The extracellular matrix of all the arches stained well with toluidine blue, with the peripheral matrix staining more intensely than that separating the cells (Figure 3.1.25). The average width of the first arch at this stage was 20.9 ± 1.0 μm (n=20), which was not significantly different than that of 20 days pf ($p = 0.77$).

Table 1 shows a summary of the cell width and cell thickness values from 13 to 20 days pf taken from the mid region of the first arch. Results of ANOVA showed a definite increase in cell width from 13 to 39 days pf ($p < 0.001$) and in cell thickness from

Figure 3.1.22
Sagittal section through the mid-ventral region of the second branchial arch of a 20 day pf embryo. Note the appearance of the newly formed hypobranchial bar (h), made up of irregularly shaped chondrocytes separated by distinct extracellular spaces compared to the branchial cartilage of the fourth arch with extracellular matrix intensely stained with toluidine blue (arrow). Epidermis (E), mitotic figure (arrowhead), perichondrium (pch), pharyngeal space (P). Bar = 10 μm

Figure 3.1.23
Sagittal section through the mid region of the fifth branchial arch of a 20 day pf embryo. Spaces between chondrocytes are difficult to resolve (arrow). Perichondrium (pch), chondrocytes (c), mitotic figure (arrowhead). Pharyngeal space (P). Bar = 9 μm


P
P
E


P

Figure 3.1.24
Sagittal section through the mid-dorsal region of the seventh branchial arch of a 20 day pf embryo showing a distinct chondrogenic (c) mid region and a prechondrogenic (pc) dorsal region. No mitotic figures seen here. Perichondrium (arrows). Pharyngeal space (P). Bar = 10 μm

Figure 3.1.25
Sagittal section through the mid region of the first branchial arch of a 39 day pf larval lamprey. The arch appears one to three cells thick. Chondrocytes (c) appear swollen, with pale-staining cytoplasm. Extracellular matrix (arrowhead) stains intensely with toluidine blue. Pharyngeal space (P). Bar = 8 μm

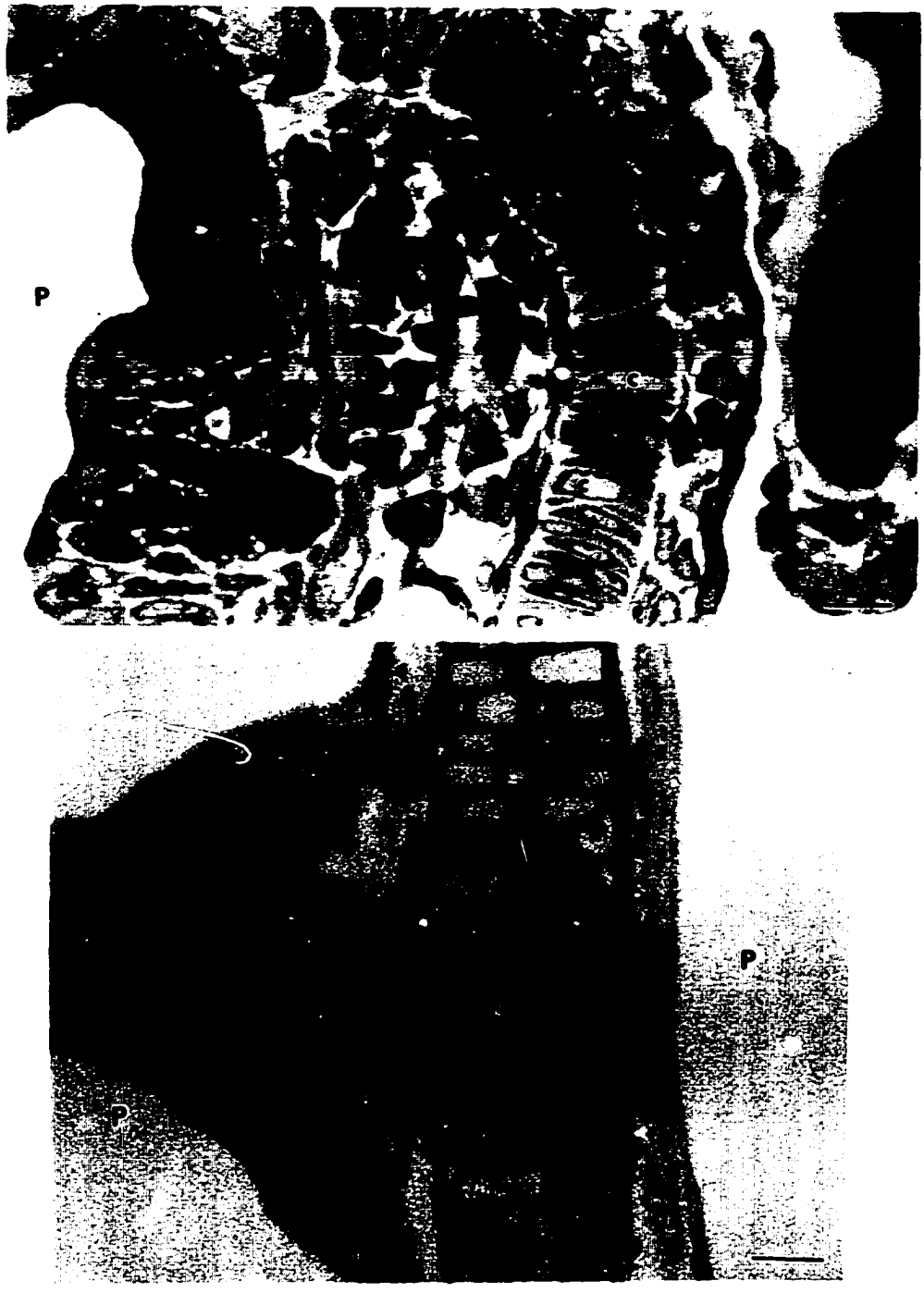
P
P
P

Table 1
A summary of the cell width and cell thickness values from 13 to 39 days pf.

Days pf	n	Cell Width [a]	Thickness [b]
13	20	17.1 ± 1.8	Not obtainable
14	20	15.6 ± 1.2*	Not obtainable
15	20	16.0 ± 1.3	1.7 ± 0.5
16	20	18.5 ± 1.3*	2.2 ± 0.4*
17	20	18.4 ± 1.2	2.3 ± 0.6
18	20	18.3 ± 1.3	Not obtainable
19	20	19.4 ± 1.6*	3.5 ± 0.6*
20	20	20.8 ± 1.2*	4.7 ± 1.0*
39	20	20.9 ± 1.0	7.4 ± 1.0*

a, b: Values are mean ± S.D. Units are μm.
* indicates value is significantly different than that preceding it (P-value less than 0.05)

15 to 39 days pf ($p < 0.001$).

3.2 HISTOCHEMICAL STAINING

The extracellular matrix (ECM) in the middle region of branchial arches 1-4 first stained with alcian blue at 16 days pf (Figure 3.2.1 A). At 17 days pf, arches 1-5 exhibited alcian blue staining in the mid regions. At 18 days pf, the dorsal and ventral regions of the first arch were staining with alcian blue. At 19 days pf, the dorsal and ventral regions of arches 1 and 2 stained with alcian blue. By 20 days pf, arches 1- 3 showed alcian blue staining in the dorsal, mid and ventral regions (Figure 3.2.1 B), and arches 4-6 were stained in the mid regions only.

Staining of the ECM with Weigert's resorcin-fuchsin was first observed at 17 days pf as a weak reaction (similar to that seen throughout most of the embryo) in the middle region of the first arch (Figure 3.2.1 C). By 18 days pf a positive reaction was seen in the middle region of arches 1 to 4, with a weak reaction observed in arch 5. This pattern of staining was similar to that observed at 19 days pf. By 20 days pf, the first arch showed a positive reaction in both dorsal and ventral regions, as well as in the mid region (Figure 3.2.1 D). Arches 2-6 were also exhibiting a positive reaction in the mid regions.

3.3 LIGHT MICROSCOPIC IMMUNOHISTOCHEMISTRY

Branchial cartilage exhibited a positive reaction when exposed to branchial matrix protein antibody in the middle region of the first arch at 16 days pf (Figure 3.3.1 A). At age 17 days pf, the middle regions of arches 1-4 reacted positively to the antibody, with

Figure 3.2.1 Histochemical staining of ECM of lamprey branchial arches. Transverse paraffin sections
A) Alcian blue 16 days pf, arch 1. B)Alcian blue 20 days pf, arch 3.
C) Weigert's 17 days pf, arch 2. D) Weigert's 20 days pf, arch 1. Chondrocytes (c), epidermis (E), pharyngeal space (P), ECM (arrows). Bar = 15 μm

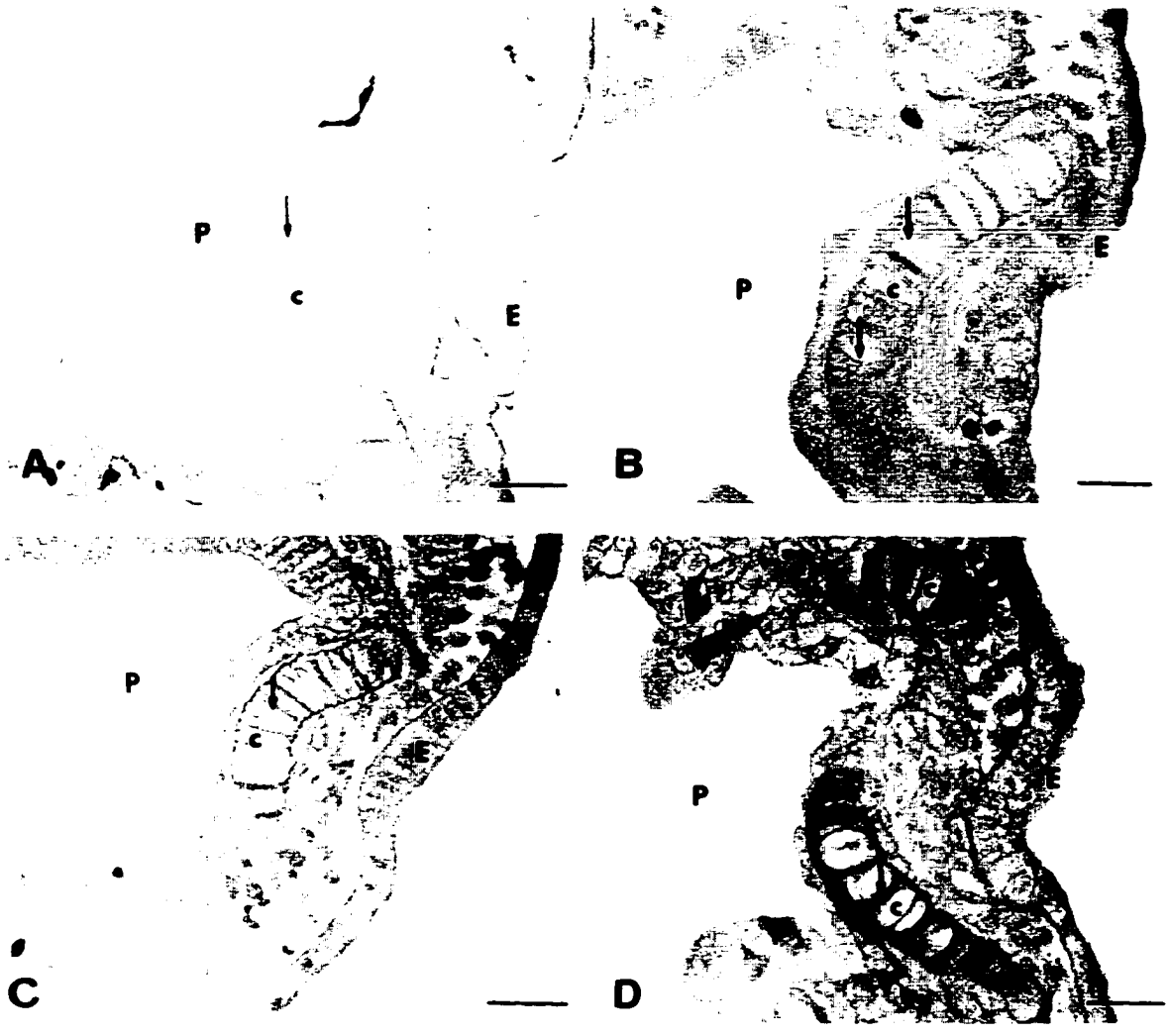
P
C
E
A
P
C
E
B
P
C
E
C
P
C
E
D

Figure 3.3.1
Immunohistochemical staining of ECM of lamprey branchial arches. Transverse sections. A) 16 days pf, arch 1. B) 20 days pf, arch 1. Chondrocytes (c), epidermis (E), pharyngeal space (P). Bar = 15 μm


P
P
E

the dorsal and ventral regions of the first arch also showing a positive reaction. At 18 days pf, the dorsal, ventral and mid regions of arches 1 and 2 reacted positively to the antibody. At 19 days pf, branchial arches 1-3 exhibited a positive reaction in the middle, dorsal and ventral regions. Arches 4 and 5 reacted positively in the middle regions. By 20 days pf, branchial arches 1-6 exhibited a strong positive reaction in the middle of the arches (Figure 3.3.1 B), as well as the dorsal and ventral regions of arches 1-4.

Table 2 summarizes the results of histochemical and immunohistochemical staining of the developing branchial cartilages.

3.4 ULTRASTRUCTURAL ANALYSIS

The first branchial arch began to form as a rod-shaped condensation of cells at 13 days pf. As viewed in lateral sections through the third pharyngeal arch, the prechondrogenic cells of the condensation were elongated and somewhat wedge-shaped (Figure 3.4.1). The cytoplasm of these cells was dense and granular with numerous ribosomes and polyribosomes (Figure 3.4.2). The most prominent organelle was the nucleus, containing many nucleoli. A few flattened saccules of rough endoplasmic reticulum (RER) containing flocculent material were scattered throughout the cytoplasm (Figure 3.4.2). Lipid droplets, some of which were very large, were also present (Figure 3.4.1). Cells were closely apposed to one another over wide areas with very little intercellular space between cells. Cells appeared to be in contact with each other via short filapodia where the extracellular spaces were dilated (Figure 3.4.2). There was no visible ECM material present between cells.

Table 2
Summary of results of histochemical and immunohistochemical staining of ECM of the developing branchial cartilages.

	Alcian Blue	Weigert's resorcin-fuchsin	Immuno-histochemistry
13 days pf	**No staining (ns)**	**ns**	**ns**
14 days pf	**ns**	**ns**	**ns**
15 days pf	**ns**	**ns**	**ns**
16 days pf	**arches 1-4**	**ns**	**arch 1**
17 days pf	**arches 1-5**	**arch 1**	**arches 1-4**
18 days pf	**arches 1-5**	**arches 1-4**	**arches 1-4**
19 days pf	**arches 1-5**	**arches 1-5**	**arches 1-5**
20 days pf	**arches 1-6**	**arches 1-6**	**arches 1-6**

Figure 3.4.1
13 days pf. Sagittal section through part of the first branchial arch precartilaginous condensation. Rectangular to wedge-shaped cells with large nuclei (N), nucleoli (n) and numerous lipid droplets (*) are tightly stacked along the dorso-ventral axis. Saccules of RER (arrowhead) are inconspicious. Bar = 2.0 μm

Figure 3.4.2
13 days pf. Sagittal section through the prechondrogenic condensation of the first branchial arch. Cells are in close apposition to each other (arrowheads) over large expanses. Note the extracellular spaces (*) which contain little to no fibrillar extracellular matrix, filapodia (arrow). Bar = 1.0 μm

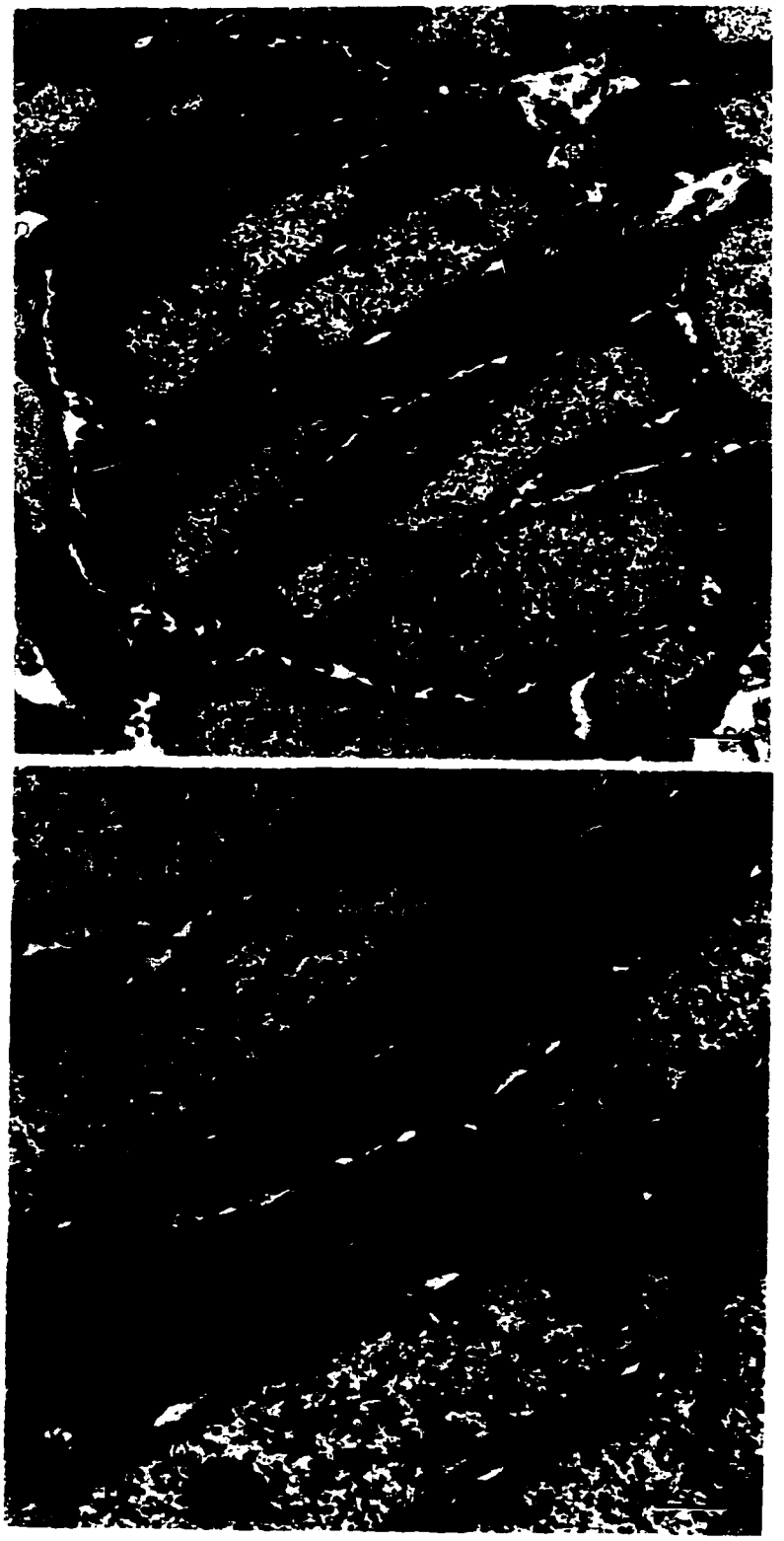

Figure 3.4.3
14 days pf. Sagittal section through the first branchial arch chondrogenic condensation. Extracellular spaces between chondroblasts or prechondrocytes are now present, although cells are still closely apposed in some areas (arrows). Bar = 2.0 μm

Figure 3.4.4
14 days pf. Higher magnification through the first branchial chondrogenic condensation. Chondroblasts (c) are partly separated from each other and the extracellular space between cells now contains a sparse beaded fibrillar material (*). RER saccules (arrowheads) containing a flocculent material similar to the ECM. Mitochondria (mi), nuclei (N). Bar = 0.5 μm

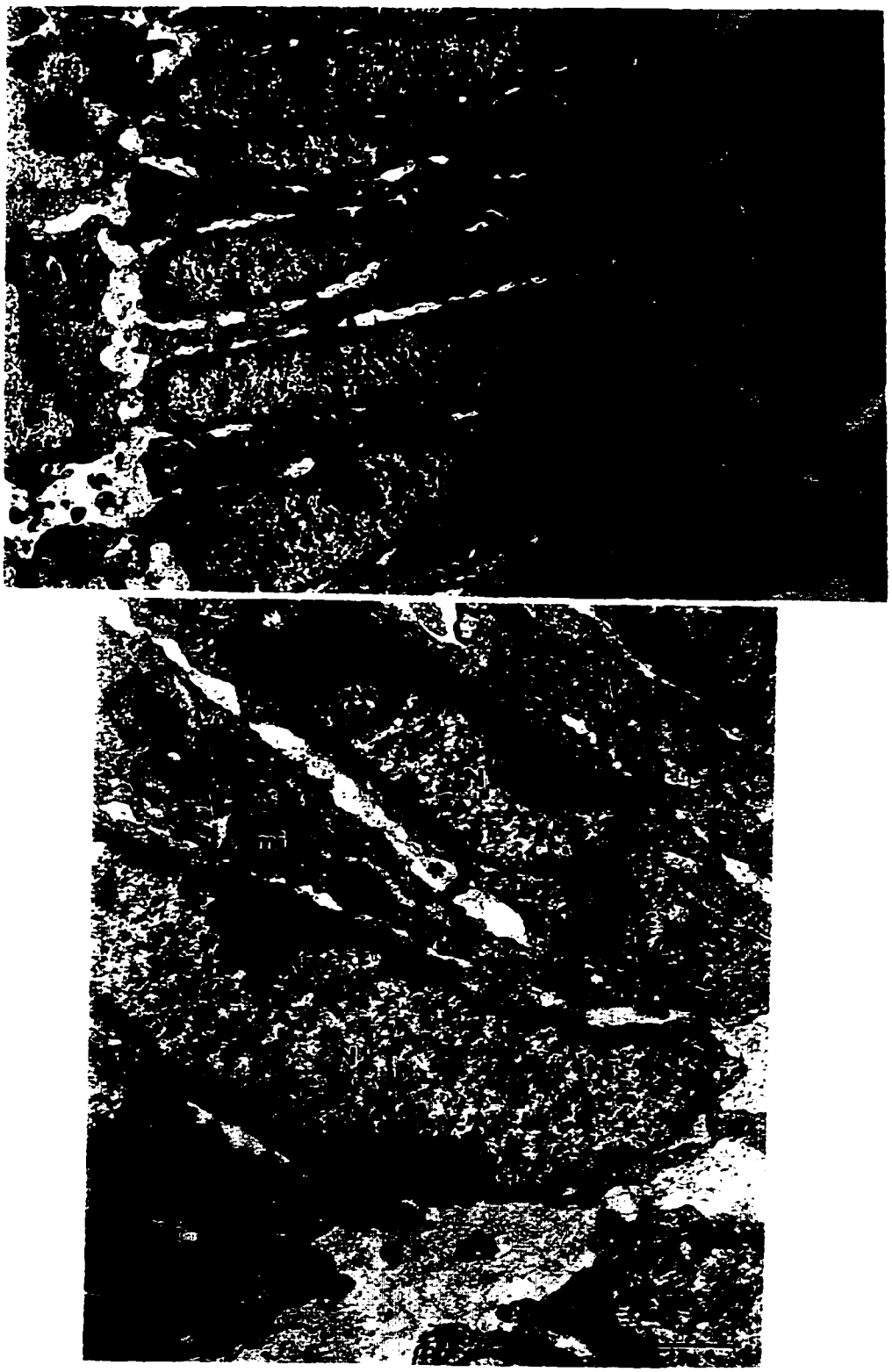

At 14 days pf, cells of the first arch resembled those seen at 13 days pf, with large nuclei and dense cytoplasm. However, saccules of the RER appeared more numerous and dilated, possessing a flocculent material (Figures 3.4.3 and 3.4.4). Cells were still in contact with each other via filapodia over wide extracellular spaces (Figure 3.4.3 and 3.3.4). At this stage, cells have begun to secrete a sparse, fibrillar extracellular matrix material and were considered chondrocytes. Most of the matrix material was located around the periphery of the condensation which resulted in a distinct separation of chondroblasts from surrounding cells.

By day 15, chondrocytes in the condensation of the first arch were separated by wide intercellular spaces which contained a sparse seam of ECM consisting of beaded, fine fibrils (Figure 3.4.5). Cells remained in contact with each other at discrete areas along the plasma membrane via filapodia. Saccules of RER containing material similar in appearance to that of the ECM were prominent features of the chondrocytes, as were lipid droplets (Figures 3.4.5 and 3.4.6).

At 16 and 17 days pf, cells in the middle region of the first arch appeared quite similar, characterized by dilated saccules of RER filled with ECM-like material. Cells were surrounded by an extensive network of beaded branched fibrillar ECM which completely separated the cells (now termed chondrocytes) from each other (Figures 3.4.7 and 3.4.8). A single layer of squamous shaped cells surrounded the new cartilage, forming the perichondrium.

At 18 and 19 days pf, chondrocytes were quite ordered in arrangement and were uniformly shaped (Figure 3.4.9). Cells had an extensive RER of dilated saccules (Figure

Figure 3.4.5
15 days pf. Sagittal section through the chondrifying first branchial arch. Chondrocytes are separate from each other except for a few focal contact points/filapodia (arrows). Extracellular matrix fibrils are present between and surrounding cells (arrowheads). Lipid (L), glossopharyngeal nerve (IX*). Bar = 2.0 μm

Figure 3.4.6
15 days pf. Sagittal section through the first branchial arch. Saccules of RER (*) are dilated and contain a material which resembles the extracellular matrix material (arrowheads).
Bar = 0.5 μm

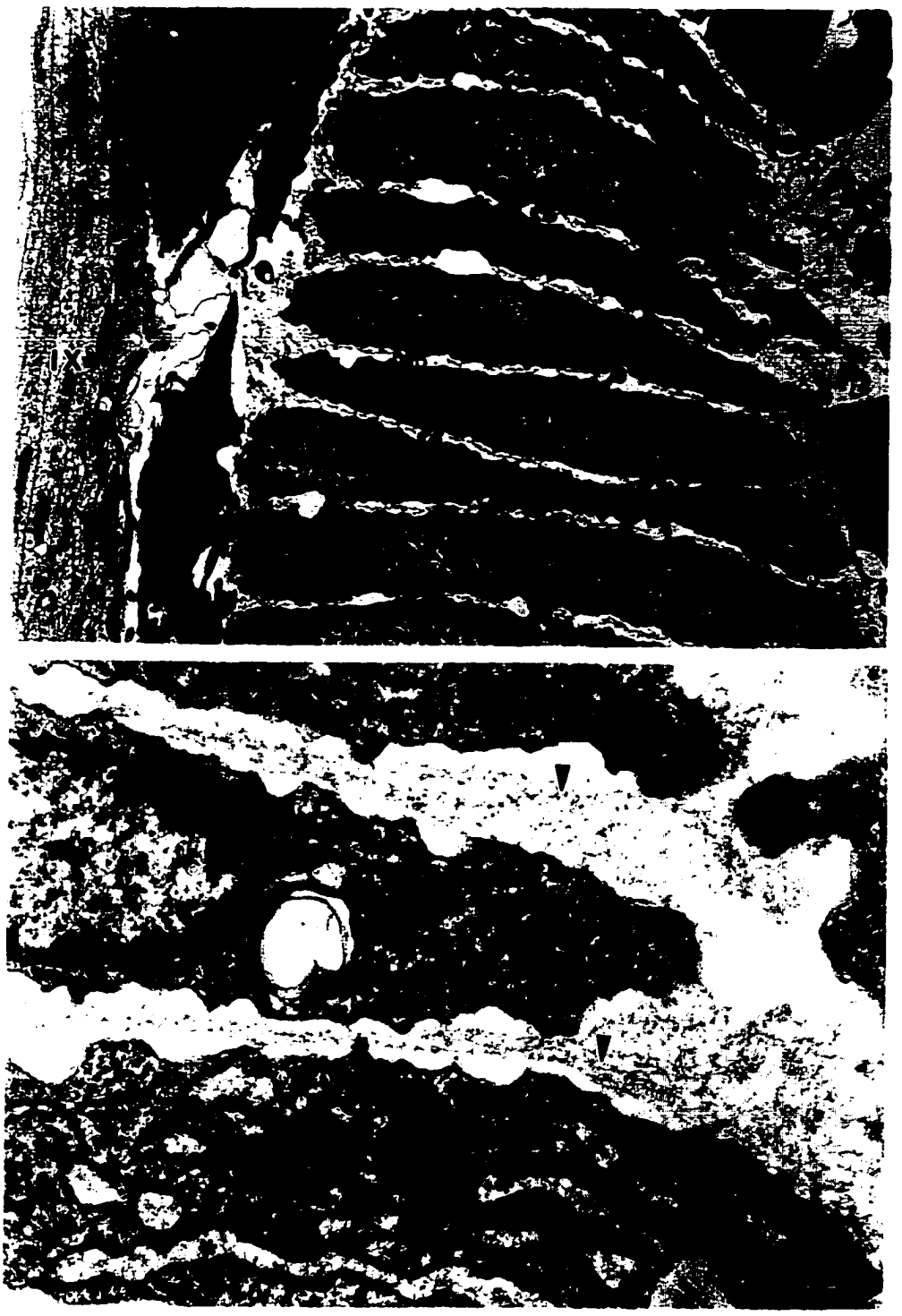

Figure 3.4.7
16 days pf. Sagittal section through the first branchial arch. Chondrocytes are well separated from each other and contain prominent dilated RER (*). Flattened cells surrounding the chondrocytes form the perichondrium (pch). Extracellular matrix (ECM) appears to have increased in density since the previous stage. Lipid (L). Bar = 1.5 μm

Figure 3.4.8
16 days pf. Higher magnification showing the density of the extensively beaded fibrillar ECM in the first branchial arch (arrowhead). Chondrocyte (c), RER (*), perichondrium (pch). Bar = 0.5 μm


ECM
L
L

Figure 3.4.9
18 days pf. Sagittal section through the first branchial arch. Note the highly ordered arrangement of uniformly shaped chondrocytes (c). The extracellular spaces between cells (arrows) are compressed and ECM (*) appears denser than in previous stages. Perichondrium (pch). Bar = 2.0 μm

Figure 3.4.10
18 days pf. Higher magnification shows the ECM (*) to be composed of a densely beaded fibrillar material. Material present in the saccules of the RER (arrowheads) resembles the ECM. Collagen fibrils are present in the periphery of the matrix (arrows). Perichondrium (pch), chondrocytes (c). Bar = 1.5 μm

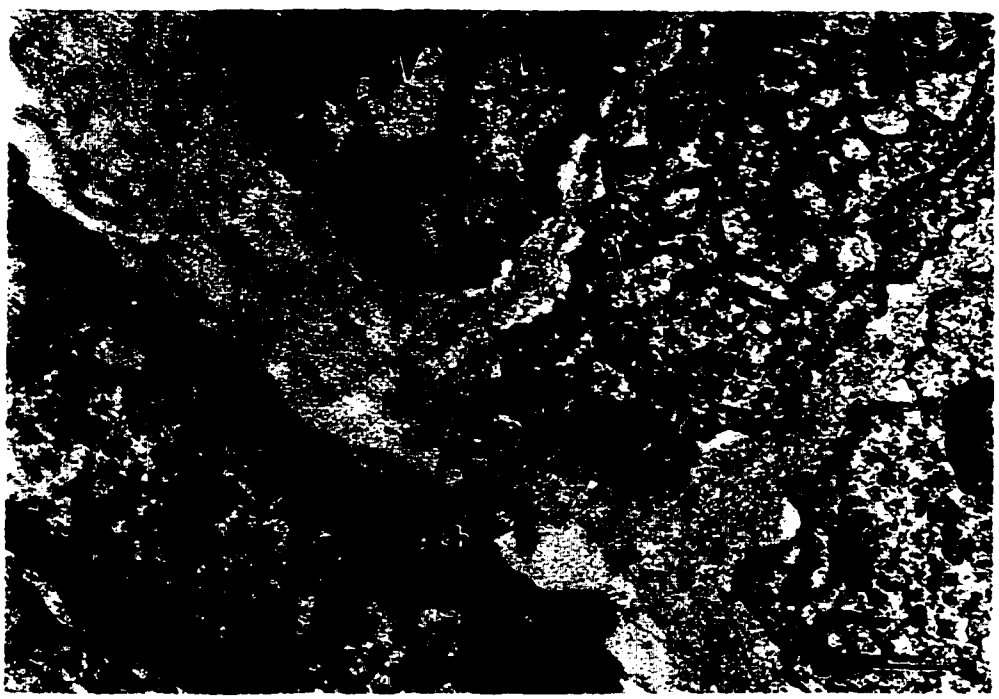

3.4.10). The space between adjacent cells appeared decreased, condensing the seams of ECM material. The ECM appeared to have increased in density in the sub-perichondral region (Figure 3.4.10). The perichondrial cells formed a flattened layer which surrounded the peripheral ECM of the branchial cartilage.

At 20 days pf, the middle region of the first arch was one to two cells thick, with cells appearing more cuboidal in shape (Figure 3.4.11). The ECM in the middle part of the arch was defined as having two zones of different densities. The sub-perichondrial region of the ECM appeared electron-lucent, consisting mainly of fine collagen fibrils closest to the perichondrium and beyond this were loosely arranged branched, beaded fibrils. The region immediately surrounding the chondrocytes was more electron dense and consisted of beaded fibrils arranged in concentric layers around the cells (Figures 3.4.12 and 3.4.13).

At 39 days pf, chondrocytes appeared quite different than those observed at 20 days pf. Cytoplasm was electron lucent, with few flattened saccules of RER. Small mitochondria were scattered throughout the cytoplasm. The ECM was arranged in 3 layers, with a territorial region immediately surrounding the chondrocytes, a more dense interterritorial region, and an electron lucent sub-perichondrial region (Figure 3.4.14).

3.5 IMMUNOELECTRON MICROSCOPY

Immunoelectronmicroscopy with antilamprey branchial matrix protein antibodies and protein A gold first showed a weak positive reaction over the ECM material at 16 days pf, indicating the presence of the branchial matrix protein at this stage (Figure 3.5.1).

Figure 3.4.11
20 days pf. Sagittal section through the mid region of the first branchial arch. ECM between and immediately around chondrocytes (*) is denser than that closer (**) to the perichondrium (pch). The arch is now one to two cells wide. Chondrocytes (c).
Bar = 3.0 μm

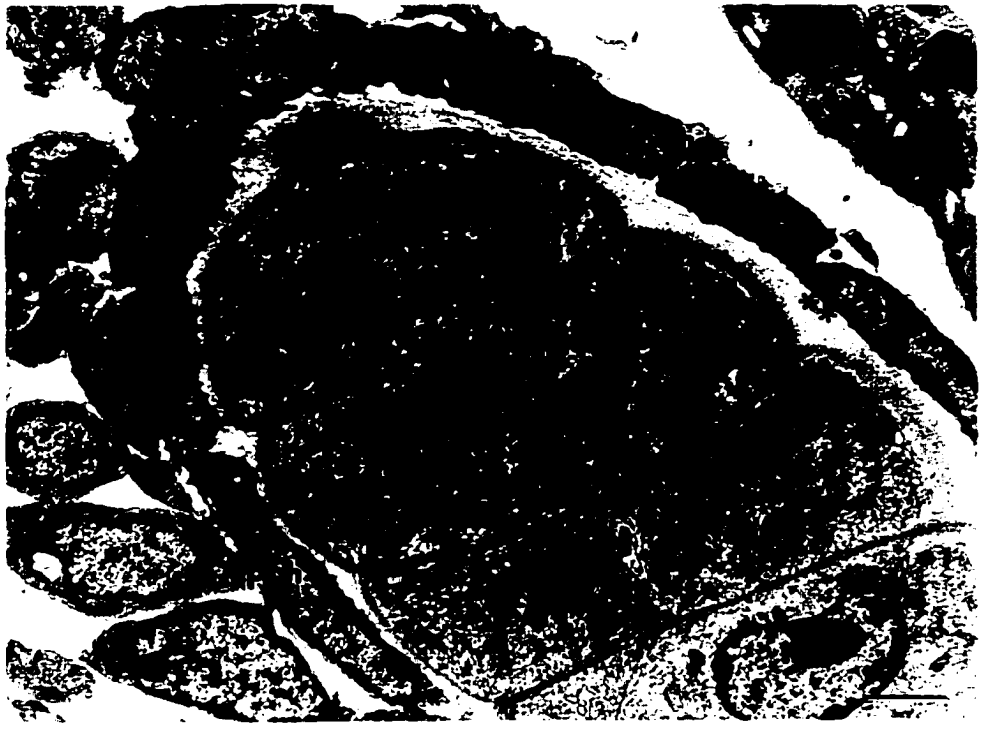

Figure 3.4.12
20 days pf. High magnification of the first branchial arch showing that the ECM is divided into two zones; the sub-perichondrial zone is electron lucent, containing fine collagen fibrils (**), and the denser region surrounding the chondrocytes consists of beaded fibrillar material arranged in layers around the cells (*). Mitochondria (mi), perichondrium (pch). Bar = 0.5 μm

Figure 3.4.13
20 days pf. Higher magnification of the extracellular matrix showing the boundary between the collagen fibrils (arrowhead) of the sub-perichondrial zone and the beaded fibrillar material of the cartilage matrix proper (*). Perichondrium (pch). Bar = 0.3 μm


mj

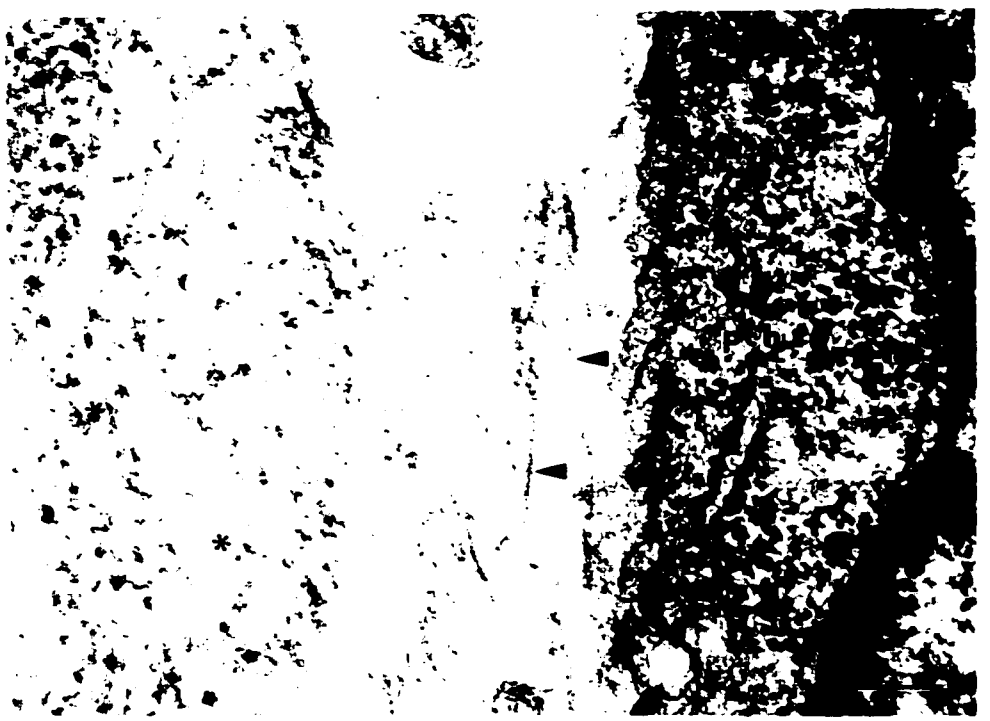
Pm

Figure 3.4.14
39 days pf. Sagittal section through the mid region of the first branchial arch. Chondrocytes have an electron lucent cytoplasm, containing few flattened saccules of RER (arrowheads). Extracellular matrix surrounding the chondrocytes consists of a dense interterritorial region (arrows) and a less dense territorial region (T). Perichondrium (pch), sub-perichondrial matrix (*). Bar = 1.0 μm

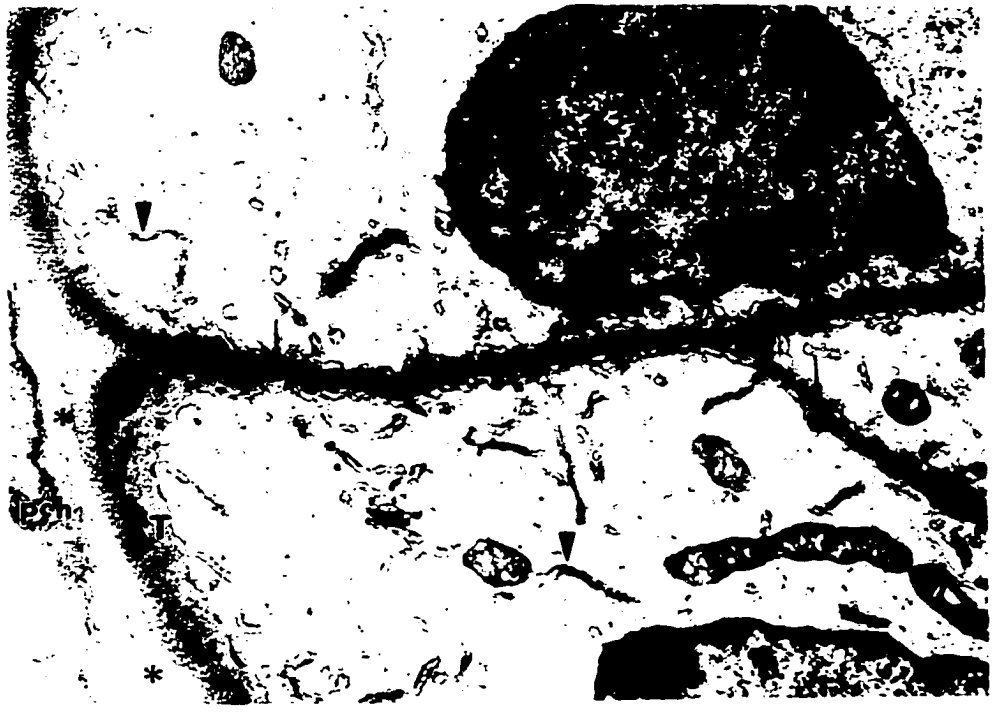
PSm
T

Figure 3.5.1
Immunoelectronmicrograph of the first branchial arch at 16 day pf, showing a weak positive reaction in the extracellular matrix to the antilamprey branchial matrix protein antibodies (diluted 1:50) labeled with protein A gold (arrowheads). Chondrocytes (c), perichondrium (pch). Bar = 0.5 μm

Figure 3.5.2
Immunoelectronmicrograph of the first branchial arch at 20 day pf, using the antilamprey branchial matrix protein antibodies (diluted 1:100) labeled with protein A gold (arrowheads). Gold particles are seen in the extracellular matrix surrounding the chondrocytes. Chondrocytes (c), perichondrium (pch). Bar = 0.5 μm

Figure 3.5.3
Immunoelectronmicroscopy on the first branchial arch of a 39 day pf larval lamprey, using the antilamprey branchial matrix protein antibodies (diluted 1:100) labeled with protein A gold (arrowhead). Gold particles are seen throughout the ECM surrounding the chondrocytes. Note high signal intensity. Chondrocytes (c), perichondrium (pch). Bar = 0.5 μm

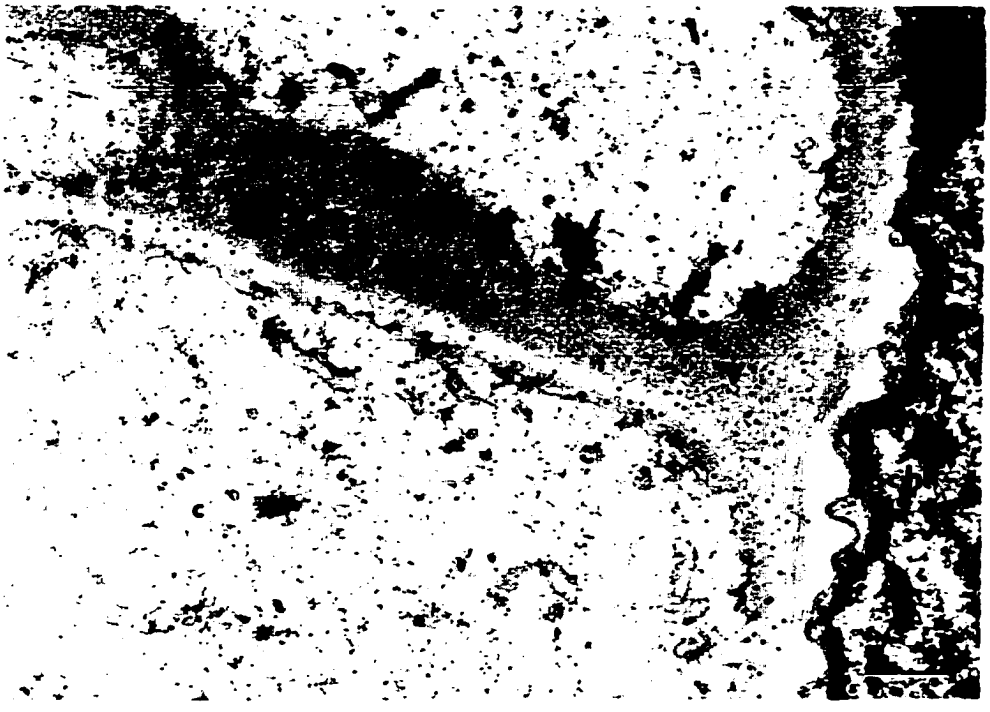

At 20 days pf, gold particles were concentrated in the dense layer of extracellular matrix surrounding the chondrocytes (Figure 3.5.2). At 39 days pf, gold labels were found throughout the ECM (Figure 3.5.3).

3.6 SUMMARY OF RESULTS

Table 3 summarizes the general morphology of the first developing branchial arch from 13 to 20 days pf. Figure 3.5.4 summarizes the morphological features associated with development of the first branchial arch from 13 to 20 days pf. Only the first arch is described, as all other arches follow the same developmental stages and are similar in morphology.

Table 3 Summary of development of lamprey branchial arches

Age	Arch 1	Arch 2	Arch 3	Arch 4	Arch 5	Arch 6	Arch 7
13 days pf	prechondrogenic						
14 days pf	prechondrogenic	prechondrogenic	prechondrogenic				
15 days pf	***chondrogenic*** mid-region extending dorsally and ventrally	***chondrogenic*** mid region	prechondrogenic	prechondrogenic			
16 days pf	chondrogenic mid-region ***perichondrium*** dorsal and ventral chondrogenic extensions	chondrogenic mid-region ***perichondrium*** dorsal and ventral prechondrogenic extensions	***chondrogenic*** mid-region ***perichondrium*** dorsal and ventral prechondrogenic extensions	***chondrogenic*** mid-region ***perichondrium*** dorsal and ventral prechondrogenic extensions	prechondrogenic		
17 days pf	chondrogenic	chondrogenic mid-region dorsal and ventral prechondrogenic extensions	chondrogenic mid-region dorsal and ventral prechondrogenic extensions	chondrogenic mid-region dorsal and ventral prechondrogenic extensions	***chondrogenic*** mid-region dorsal and ventral prechondrogenic extensions	prechondrogenic	
18 days pf	chondrogenic two rod shaped anterior projections	chondrogenic mid-region	chondrogenic mid-region	chondrogenic mid-region	chondrogenic mid-region ***perichondrium***	***chondrogenic*** mid-region ***perichondrium***	
19 days pf	chondrogenic	chondrogenic mid-region	chondrogenic mid-region	chondrogenic mid-region	chondrogenic mid-region	chondrogenic mid-region	
20 days pf	loop around 1st gill opening 1-2 cells wide	two rod shaped anterior projections	two rod shaped anterior projections	two rod shaped anterior projections	two rod shaped anterior projections	two rod shaped anterior projections	***chondrogenic*** mid-region dorsal and ventral prechondrogenic extensions ***perichondrium***

Figure 3.5.4 Diagram summarizing the morphological features during chondrogenesis of the first branchial arch. A) 13 days pf. Wedge-shaped prechondrocytes or chondroblasts are orderly arranged, and very closely apposed to each other. B) 15 days pf. Chondrocytes in the mid region are well separated from each other by complete extracellular spaces between cells. The dorsal and ventral regions of the arch consist of closely packed prechondrocytes. C) 18 days pf. Cells in the mid region of the arch have increased in size, and cell boundaries are hard to distinguish. These cells are very uniformly shaped. Chondrocytes in the dorsal and ventral regions are separated by complete extracellular spaces. D) 39 days pf. Chondrocytes are separated by an extracellular matrix which stains intensely with toluidine blue. Cytoplasm is pale. The arch is now 1-3 cells wide.

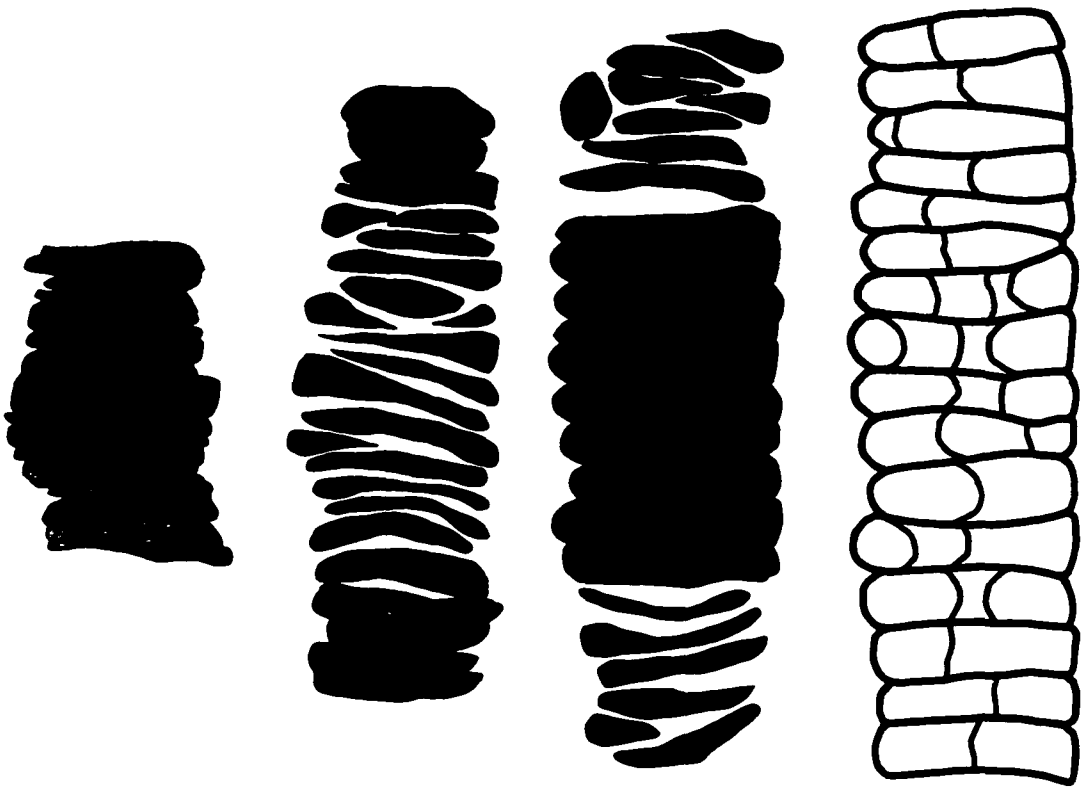
A
B
C
D

4. DISCUSSION

The main purpose of this study was to define the spatial and temporal pattern of lamprey branchial cartilage development using high resolution light microscopy (HRLM) and transmission electron microscopy (TEM). This extensive examination of chondrogenesis defines a set of well characterized morphological features that will be utilized in future investigations of the molecular aspects of lamprey branchial cartilage development.

4.1 FIRST BRANCHIAL ARCH

Branchial cartilage chondrogenesis begins in embryonic lamprey at 13 days pf with the formation of the first branchial arch as a dorsoventrally aligned rod-shaped precartilage condensation. Cartilage differentiation or chondrification, defined by the presence of the unique fibrillar protein characteristic of branchial cartilage in the ECM, is first observed within the first arch at 14 days pf. As differentiation proceeds, mesenchymal cells from the dorsal and ventral regions of the pharyngeal arch form two new precartilage condensations which are in continuum with the middle chondrifying region, extending the first branchial arch both dorsally and ventrally. Differentiation of the ventral and dorsal regions proceed similar to the mid region of the arch. As chondrocyte differentiation proceeds, the cells enlarge and are separated by the accumulating fibrillar ECM.

4.2 OTHER ARCHES

All branchial arches follow the same general pattern of development as the first arch. Although arches 1-4 are present by 15 days pf, only the first and second are chondrogenic, with arches 3 and 4 present as prechondrogenic condensations. Arches 5 and 6 appear as precartilage condensations on days 16 and 17 pf respectively. Branchial arch 7 is the last to form but develops rapidly, first visible at day 20 pf in a chondrogenic state. Arches are present in a gradient of developmental maturity, with the first being the most advanced and the seventh the least. By day 16 pf, a perichondrium appears associated with the mid region of the first branchial arch and may be a source of cells for appositional growth. A perichondrium appears in association with arches 2-7 as they chondrify.

4.3 SPATIAL DEVELOPMENT

4.3.1 Condensation

Lamprey branchial cartilage, like primary cartilages of both higher and lower vertebrates, develops from precartilage condensations. A condensation stage is also found in the development of other vertebrate tissues, such as teeth, feathers, hair, muscles, tendons and ligaments (Solursh and Reiter, 1980; Hall and Miyake, 1992). A condensation allows aggregations of like cells to come into contact with each other (Thorogood and Hinchliffe, 1975; Solursh and Reiter, 1980; Hall and Miyake, 1992). This may be important in: 1) reducing intercellular distances to increase cell-cell contact and allow the formation of gap junctions or 2) in increasing the gradients of diffusible

influences, such as growth factors which are required for cartilage development (Hall and Miyake, 1995; Wezeman, 1998). Gap junctions may be important in facilitating the direct transfer of cAMP from cell to cell, an intercellular molecule that has been implicated in the regulation of limb cartilage differentiation in chicks (Coelho and Kosher, 1991).

Condensations form by one or more of the following: 1) an increase in mitotic activity in comparison with non-condensing mesenchyme, 2) aggregations of cells toward a center and/or 3) failure of cells to move away from a center (Ede, 1983; Hall and Miyake, 1992; Hall and Miyake, 1995). In the lamprey branchial chondrogenesis, mitotic figures were not prominent during the condensation stage. It appears that condensations in this case form as a result of mesenchymal cell aggregation toward a center. This differs from lamprey trabecular cartilage, where numerous mitotic figures are seen during the condensation stage, suggesting that cell proliferation is mainly responsible for forming the condensation (McBurney and Wright, 1996).

Precartilage condensation formation is often dependant on an early interaction of prechondrogenic mesenchymal cells with epithelium (Solursh, 1983; Hall and Miyake, 1995). In the lamprey trabecular cartilage, it is presumed that contact between the ventromedial mesenchymal cells of the trabecular arc and the basal lamina of the buccal epithelium may be essential for the formation of the trabecular condensation (McBurney and Wright, 1996). Cell interactions between pharyngeal endoderm and neural crest are believed to be necessary for the development of branchial cartilages in lamprey (Damas, 1944; Newth, 1956). In support of this, the present study has found that in early stages of lamprey embryonic development, the mesenchymal cells from which prechondrocytes

will form are in very close apposition to the pharyngeal epithelium.

The normal duration of a condensation in skeletogenesis of mammals and birds is about 12 hours (Hall and Miyake, 1995). However, in some cases, such as in the elastic cartilage of the rat ear, the condensation stage can persist for 14 days (Hall and Miyake, 1995). The rapid (12 hour) transition from precartilage to cartilage may be due to the fact that most of the cartilaginous structures that form in mammals and birds constitute a chondrogenic skeletal template which then must undergo osteogenesis to become bone. Therefore, the condensation process must be rapid to allow for the formation and growth of the cartilaginous template and, in some cases, its transition into bone during embryonic life. In the lamprey, condensations of the trabecular cartilage lasted for about 2 days, beginning at day 17 pf and ending with the secretion of lamprin ECM at day 19 pf (McBurney and Wright, 1996). In the case of lamprey branchial cartilage, condensations were generally present from 24 to 48 hours before distinct extracellular spaces containing the fibrillar ECM appeared between cells, indicating differentiation (ie. chondrification). These condensations in the lamprey were found to last longer than the typical duration of 12 hours in the birds and mammals, possibly due to the fact that the skeleton of the lamprey remains cartilaginous throughout life, and therefore does not need to differentiate further (i.e. osteogenesis).

Unlike those of other vertebrate precartilage condensations, including lamprey trabecular cartilage, the cells in the precartilage condensations during lamprey branchial development are arranged in a relatively orderly, stacked array. Kimmel *et al.* (1998) assumed that the orderly stacks of cells that emerge during chondrification of pharyngeal

cartilage in zebrafish, *Danio (Brachydanio) rerio*, originate from condensations of cells in a disorderly array. However, they did not look at precartilage condensations. It is possible that the orderly stacks of chondrocytes observed in the zebrafish originate from an orderly array of prechondrocytes, as was found in the lamprey. However, Meckel's (mandibular) cartilage in the Cichlid fish *Hemichromis bimaculatus* originates from a disorderly condensation of closely packed pyramidal shaped prechondrocytes (Huysseune and Sire, 1992). According to the same authors, these cells become arranged in an ordered fashion only when they are chondrogenic.

The development of the lamprin-based trabecular cartilage in the embryonic lamprey (McBurney, 1995; McBurney and Wright, 1996) and piston cartilage during metamorphosis of the lamprey (Armstrong *et al.*, 1987) exhibit a pattern of arrangement and development similar to that of limb buds in birds and mammals. Precartilage condensations in developing limb buds originate from a core of rounded cells in the center of the limb bud (Wezeman, 1998). Other cells aggregate around this core, forming a whorling pattern of rounded prechondrogenic cells. Chondrification begins in the centre of the condensation and proceeds centrifugally (Wezeman, 1998). In contrast to these condensation patterns, the flattened cells of the branchial precartilage condensation in lamprey are stacked in a pile one cell wide and remain in this orderly array throughout development.

During condensation in chick limb development, cell densities increase continuously, peaking immediately prior to chondrification or overt cartilage differentiation (Thorogood and Hinchliffe, 1975; Ede, 1983). This peak is one of the

characteristics of the condensation process. A measurement of cell densities during development of lamprey trabecular cartilage showed two peaks; one at day 16 pf prior to the initial appearance of condensations, and another at day 18 pf, just before cartilage differentiation (McBurney and Wright, 1996). McBurney and Wright (1996) suggested that the first peak, occuring at the precondensation phase, could be due to cell proliferation and/or a reduction in the amount of intracellular yolk in the cells, and thus cellular volume. Although cell densities were not measured during lamprey branchial cartilage development, visual observations of the condensation and chondrogenic events suggest that only one peak in cell density occurs prior to chondrification and ECM deposition. This corresponds to what occurs in avian and mammalian limb bud chondrogenesis (Thorogood and Hinchliffe, 1975; Ede, 1983).

4.3.2 Cell Differentiation

With condensation, there is a change in cell shape and ultrastructure (Wezeman, 1998). When avian and mammal limb bud mesenchymal cells first condense, they pull in their filapodia and become rounded in shape. They have a high nucleo-cytoplasmic ratio, large nucleoli, numerous mitochondria, poorly developed endoplasmic reticulum, and numerous ribosomes (Thorogood and Hinchliffe, 1975; Hall and Miyake, 1992; Wezeman, 1998). As precartilage cells differentiate into chondroblasts, the RER increases in size, indicating protein synthetic activity in the cell (Stockwell, 1979). Although cells making up branchial precartilage condensations in lamprey appear flattened and disc-shaped rather than round, they exhibit the same ultrastructural characteristics as those

described for mammalian and avian limb bud cartilages. The dilated cisternae of the RER contain material similar to that found in the extracellular space. Numerous lipid inclusions are also seen in precartilaginous condensations, and as the chondroblasts develop, lipid content seems to decrease. However, lipids do not disappear, as they are present in adult branchial cartilage (Wright *et al.*, 1988). It has been hypothesized that the lipids in chondroblasts of developing elastic cartilage in rat ears are metabolized during the early post-natal period of intensive synthetic activity (Kostović-Knežević *et al.*, 1986). I believe that the same thing happens in lamprey, as the lipid content appears to decreases as cells differentiate and begin to secrete ECM.

Both lamprey trabecular and branchial arch cartilages originate from neural crest cells (Langille and Hall, 1988). The cells that migrate to form the trabecular cartilage originate from the neural crest at the level of the posterior prosencephalon to the mid-rhombencephalon. Those cells that form the branchial cartilage originate from the neural crest at the level of the mesencephalon to the level of the fifth somite (Langille and Hall, 1988). These two populations of neural crest cells overlap from the posterior mesencephalon to the mid rhombencephalon. Yolk is prominent in neural crest cell-derived mesenchyme from which the trabecular cartilage condensations form (McBurney, 1995; McBurney and Wright, 1996). Yolk is not present in cells forming branchial precartilage condensations. This difference in cell morphology during early stages of trabecular and branchial cartilage development may indicate that the originating populations of neural crest cells differ in their yolk content.

4.3.3 Differentiation patterns

All lamprey branchial arches follow the same pattern of development, appearing first as small rod-shaped prechondrogenic condensations. As the cells in this condensation differentiate into chondrocytes, two other precartilage condensations form; one dorsal and one ventral to the original condensation. These two new condensations then undergo chondrification to form one elongated cartilaginous arch. The formation of one continuous cartilaginous structure from the fusion of two precartilage condensations to a third chondrifying portion is unlike what has been described in other vertebrates. In fish, birds and mammals, there can be more than one site of chondrification within one single condensation, with cells existing in regions that remain at the condensation stage for different periods of time. These chondrification sites may then all fuse to form one cartilaginous structure or separate to form different cartilage structures (Hall and Miyake, 1995; Kimmel *et al.*, 1998).

In light of the present study, it would appear that the pattern of lamprey branchial arch chondrogenesis may be ancestral to that of chondrichthians and osteichthyes. Analysis of the developing branchial cartilages of the zebrafish by Schilling and Kimmel (1997) revealed that a branchial arch initially consists of a single condensation and that subdivisions of the one condensation results in the formation of dorsal and ventral sets of cartilages. This pattern of chondrification results in teleost and chondrichthian branchial arches being made up of five different cartilaginous structures: the dorsal pharyngobranchials and epibranchials, the middle ceratobranchials, and the ventral hypobranchials and basibranchials (Cubbage and Mabee, 1996; Shilling *et al.*, 1996).

These five structures articulate with each other to form one arch. In the lamprey, the branchial arch is made up of only one structure with no articulations which develops from three different but continuous condensations. The slower-developing dorsal and ventral condensations, which are continuous with the middle, more developed condensation, may have given rise to the two dorsal and two ventral structures in chondrichthians and teleosts due to changes in developmental timing or heterochrony. Heterochrony is a shift in the relative timing of two developmental processes during embryogenesis (Gilbert, 1997). For instance, if a shift in the timing of the formation of the dorsal and ventral condensations of the lamprey branchial arches appeared after the middle region of the arch was surrounded by a perichondrial layer and differentiated into cartilage, the condensations could presumably result in two separate cartilaginous structures that would not be continuous with the mid region. This pattern of development might lead to the presence of articulated elements similar to those of the teleost branchial arches.

Studies of the organization and division of chondrocytes during hyoid arch formation in the zebrafish show that the arch consists of a large plate-like region and a rod-like extension (Shilling and Kimmel, 1997; Kimmel *et al.*, 1998). The rod-like anterior end of the developing hyoid arch is made up of chondrocytes that are extremely flattened, becoming thicker as the cartilage matures. This flattened arrangement of cells is the result of compression as new cells are added via mitosis to the base (posterior end) of the rod, near the plate region (Kimmel *et al.*, 1998). This mechanical flattening of the chondrocytes does not occur in lamprey branchial cartilage where cells are recruited to the condensation from the surrounding mesenchyme. There is no apparent compression

forcing the cells into a flattened arrangement.

Chondrogenesis has been widely studied using developing chick limb buds (Hall and Miyake, 1995). Skeletal elements of the chick hind limb each form from one condensation and cells are arranged in the condensations so that some are at a later stage of development than others. For instance, the Y-shaped condensation that forms the femur, tibia and fibula contains a gradation of cell differentiation, with the most proximal cells being surrounded by matrix (therefore termed chondrocytes), and the more distal cells still in contact with each other with no discernable ECM (therefore still considered prechondrocytes) (Thorogood and Hinchliffe, 1975; Ede, 1983). Thus differentiation of each piece of cartilage in the chick limb proceeds only in one direction within each condensation. In contrast to this, the lamprey branchial cartilage exhibits simultaneous differentiation within each condensation.

4.3.4 Extracellular matrix (ECM)

As previously mentioned, lamprey branchial and pericardial cartilages differ from lamprin-based trabecular, annular and piston cartilages in their ECM composition. Branchial cartilage in the lamprey contains a unique extracellular matrix protein which is similar in some respects to elastin (Robson *et al.*, 1997).

As branchial chondroblasts mature, they are pushed apart by accumulating ECM. The first ECM material secreted at 14 days pf consists of a beaded fibrillar material, along with few collagen fibrils. It is not known whether the collagen fibrils are secreted by the chondroblasts or the peripheral undifferentiated mesenchymal cells. As chondrification

proceeds, the ECM can be divided into two zones of different densities, the sub-perichondrial zone contains a fibrillar ECM consisting of collagen fibrils and the region immediately surrounding the chondrocytes (territorial) contains the major ECM protein, present as a dense, beaded fibrillar material arranged in rings around the chondrocytes and no collagen fibrils. A similar concentric ring pattern of ECM arrangement is also seen in the anterior and middle lingual cartilage of the hagfish (Wright *et al.*, 1998).

At 39 days pf, young larval lamprey branchial cartilage ECM is divided into three regions: a territorial region, a denser interterritorial region, and an electron lucent sub-perichondrial region. This is similar to the adult lamprey branchial cartilage only in that there are three ECM layers. In adult branchial cartilage, the sub perichondrial region consists of a dense layer of coalesced matrix fibrils, the pericellular region (immediately surrounding the chondrocytes) consists of matrix granules and a fine filamentous material, and the interterritorial region consists of loosely arranged branched fibrils and coalesced seams of matrix (Wright *et al.*, 1988). Matrix fibrils in adult branchial cartilage are not arranged in rings around the chondrocytes.

In comparison, the ECM components in the hyaline cartilage of the embryonic chick limb is organized into two regions: the region which immediately surrounds the chondrocytes is made up of a network of beaded strands and dense granules (proteoglycans) and the region surrounding this consists of electron-dense amorphous material and banded collagen type II fibrils (Wezeman, 1998). In adult gnathostome hyaline cartilage, the territorial matrix is characterized by a finely textured ECM containing a meshwork of unbanded filaments and an absence of banded collagen fibres,

and the interterritorial matrix is made up of the major ECM protein of hyaline cartilage, collagen type II (Stockwell, 1979). The subperichondrial region of type I collagen fibrils merge with type II fibrils of the interterritorial matrix.

4.4 TEMPORAL DEVELOPMENT

4.4.1 Timing of cartilage appearance

In the lamprey, the branchial arches are the first cartilaginous structures to form, followed by the trabecular cartilage (Damas, 1944). The arches appear in order, from cranial to caudal. At stage 16 (Gill cleft: day 15-17 pf) gill slits appear and start to function (Piavis, 1961). Results from this investigation demonstrate that branchial arches are first present at 13 days pf (stage 15) and that by days 15, 16 and 17 pf (stage 16), branchial arches 1-4, 5 and 6 respectively are already in place and are in various stages of differentiation. Since the arches provide a supportive function for the pharyngeal wall and a site of muscle attachment which are both necessary for respiratory function, it is presumed that they must develop before respiration can occur through the gill slits. The trabecular cartilages, which are first present at 17 days pf and cartilaginous by day 19-20 pf (Stage 17: Burrowing) (McBurney, 1995), provide support for the brain and are not needed prior to the burrowing stage (17-33 days pf).

Like the lamprey, the skeletal structures of the teleost skeleton appear as they are needed for the survival of the fry. However, the development of the teleost cranial skeleton begins before and during hatching with the trabecular cartilage forming before the branchial arches (Smith, 1960; Vandewalle *et al.*, 1992; Shilling and Kimmel, 1997).

The reason that the branchial cartilage develops after the trabecular may be due to the fact that, in teleosts, respiration prior to and during hatching takes place through the skin and yolk sac and therefore gill development is not an immediate priority. As the yolk sac decreases in volume, the branchial system takes over respiration and at this point, branchial arch support would be necessary (Vandewalle *et al.*, 1992). Lamprey embryos hatch at 10-13 days pf. Since lamprey do not possess a yolk sac at hatching, the post hatch lamprey embryo must quickly develop the supportive branchial arches and gills to obtain sufficient levels of oxygen.

4.4.2 Previous studies

The development of the lamprey head skeleton has been studied by Damas (1944), Johnels (1948) and DeBeer (1971) using paraffin-embedded material and routine histological staining. These early studies on *Lampetra* species provided an overview of many developing structures in embryonic lamprey but did not concentrate specifically on the branchial cartilages. In addition, the limited technology available at the time has left gaps in our understanding of branchial cartilage development. Since lamprey embryos used in these earlier studies were not raised in controlled laboratory conditions, it is also difficult to compare timing of developmental events. In addition, the terminology used to describe development is confusing and sometimes difficult to equate with modern nomenclature and knowledge of chondrogenesis. My HRLM and TEM analysis of a series of staged embryos raised in controlled conditions has allowed a detailed study of lamprey branchial chondrogenesis from beginning to end.

The present investigation demonstrates that the precartilage condensation of the first branchial arch is visible early in stage 15, at day 13 pf. This correlates with the observations of Damas (1944) who describes the beginning of the first branchial arch as a "rounded mass of swollen cells" in embryos of *L. fluviatilis* comparable to stage 15 (13-16 days pf) in *P. marinus*. Johnels (1948) also notes the presence of the first branchial arch at 365 hrs (15 days) in L. *fluviatilis*, although he describes it as a small rod of procartilage. Presumably procartilage means chondrifying tissue, since a precartilage condensation in 1948 would have been referred to as a blastema. DeBeer (1971) was the first to summarize and depict all the developing branchial arches in a series of embryonic lamprey (*L. planeri*) defined as being early stage, 24, 25, 26 and 45 days. According to DeBeer (1971), six arches are present at an early (undefined days pf) stage as slender vertical struts of procartilage. Presumably here procartilage is equivalent to precartilage condensations since at 24 days, he states the 6 arches are chondrified and becoming curved and the 7th arch is mesenchymatous. Our study has shown that six arches are present in varying degrees of development at 17 days pf, and as seen from the 3-D reconstruction (Figure 3.1.11), show varying degrees of curving. By 20 days pf, all arches are present and chondrified.

4.4.3 Extracellular matrix

Lamprey cartilages are either lamprin-based (as is the trabecular cartilage) or composed of an as yet unnamed distinct form of non-collagenous elastin-like protein (as is the branchial cartilage). Gnathostome cartilages are collagen-based and type II collagen

secretion is considered a major early marker of chondrocyte differentiation (Eliebacker *et al.*, 1995). In higher vertebrates, mRNAs for collagen type II and other cartilage specific proteins are present prior to precartilage condensation and up-regulated during condensation, while protein products of these mRNAs accumulate only as chondrification proceeds (Hall and Miyake, 1995). In lampreys, both lamprin mRNA transcripts and lamprin fibrils are first detected in trabecular cartilage at the beginning of chondrification (McBurney *et al.*, 1996b). The first presence of matrix material at day 14 pf marks the beginning of chondrification of the first branchial arch in lamprey. Immunohistochemical and immunoelectronmicroscopic analysis first identified the branchial ECM protein at day 16 pf. The failure to identify matrix protein at 14 days pf may be due to the limited sensitivity of the immunocytochemical procedures on paraffin and resin sections and the small quantities of matrix material present at that time. Once the branchial matrix protein is characterized, *in situ* hybridization will be utilized to establish when the transcripts for the branchial protein are present.

Alcian blue (pH 2.5) is a common marker for differentiating (chondrifying) vertebrate cartilage, binding to carboxyl and sulphate-ester groups located on the proteoglycans in the ECM. Differentiating cartilaginous structures in zebrafish are characterized by weak, variable staining initially, followed by more intense staining as the cartilage matured (Shilling and Kimmel, 1997). In our study, proteoglycans were present in high enough concentrations in chondrifying branchial arches 1-4 at 16 days pf to stain weakly with alcian blue, with the intensity of stain increasing as cartilage matures.

The matrix of the first arch stains weakly with the elastin stain Weigert's resorcin-

fuchsin at 17 days pf and by 18 days pf, arches 1-5 stain adequately. It is not known exactly what this stain binds to, only that it is specific to elastin and that it reacts specifically with adult and larval lamprey branchial cartilage (Wright, unpublished data). Since this reaction first takes place only at 17 days pf, it is not as sensitive as immunohistochemistry or immunoelectronmicroscopy in detecting the presence of branchial ECM protein.

4.4.4 Cartilage growth

Cartilage growth may be achieved in 4 ways: cell recruitment from surrounding tissues, cell division, cell enlargement and matrix secretion (Hinchliffe and Johnson, 1983).

In lamprey, although the first precartilage condensation of each arch is distinguishable from the surrounding mesenchymal cells, the boundary separating the ends of the dorsal and ventral condensations are difficult to distinguish from the mesenchyme in these regions, suggesting cell recruitment may contribute to growth of these two precartilage condensation. Based on the lack of mitotic figures, there appears to be very little cell division during condensation and early chondrification in lamprey branchial cartilage. The prevalence of mitotic figures by day 19, after chondrocytes had differentiated, suggests that some cartilage growth at this stage is due to cell proliferation or interstitial growth. Intercalated cells between chondrocytes may indicate cell recruitment from the perichondrium contributing to growth during differentiation.

Cell enlargement contributes in a small way to the growth of lamprey branchial

cartilage. Measurements of cells thickness in the differentiating cartilage of the first branchial arch indicate a slight increase in cell thickness and diameter with age. The average thickness of cells increases with age, and at 19 days pf, chondrocytes are significantly thicker (67%) than those of 17 days pf. Chondrocytes also increase slightly in diameter with age, with cells at 20 days pf significantly wider (9%) than those at 16 days pf. Matrix secretion may also play a small role in the growth of the branchial cartilage. Intercellular spaces containing ECM appear to increase in width between cells until about 17 days pf. At 18 days pf, the intercellular spaces appear to have decreased in width as the chondrocytes become thicker and the matrix becomes compact. Hence, within the confines of this study, matrix secretion and cell migration appear to play a role in branchial cartilage growth at early differentiation stages, with cell enlargement and cell proliferation contributing to growth at later stages.

The coin-like shape and arrangement of cells in a stack during branchial cartilage development may facilitate the direction of growth. A similar cell arrangement and shape is found in the cartilage of filament spines of teleost gills, which allows for growth in length of the gill filament along the long axis of the filament spine (Benjamin, 1990).

5. SUMMARY

Branchial cartilage chondrogenesis begins in embryonic lamprey at 13 days pf. Cartilage differentiation, defined by the presence of the unique fibrillar protein characteristic of branchial cartilage in the ECM, is first observed within the first branchial arch (3rd pharyngeal arch) at 14 days pf. Chondrogenesis of the lamprey branchial

cartilage is unique in that mesenchymal condensations first appear in the mid-region of pharyngeal arches 3-9 as a one-cell wide orderly stack of flattened cells, and this condensation is extended by the addition of two new condensations, one dorsally and one ventrally. Lamprey cartilage condensations last for about 24 to 48 hours. When the precartilage dorsal and ventral condensations appear, the mid region of the arch is chondrogenic. This process is different than what occurs in teleost gill arches, where more than one skeletal element forms from a single condensation (Hall and Miyake, 1995; Kimmel *et al.*, 1998). As chondrogenesis proceeds, cells grow in size and are separated by accumulating ECM.

In contrast to other vertebrate cartilage condensations, prechondrocytes in the lamprey branchial cartilage are arranged in an orderly array. Cells remain stacked in an orderly array throughout development. Once the condensations start to undergo chondrogenesis, the branchial arches begin to grow. At early differentiation stages, growth occurs as a result of matrix secretion and cell migration. At later stages in development, the arches grow mainly by cell enlargement and cell proliferation.

In lamprey, patches of ECM material identified at 14 days pf mark the beginning of chondrification of the first branchial arch. Matrix material appears to increase in quantity and density until day 20 pf, where it is organized into two zones of different densities, the sub-perichondrial zone (which contains collagen fibrils) and the territorial zone, which contains the unique branchial ECM protein. This protein appears as beaded strands which are arranged in rings around the chondrocytes.

In order to fully understand the importance of this unusual cartilage, additional

studies must be carried out to identify more characteristics of the ECM protein. Based on the present study, the branchial ECM protein is detectable at 16 days pf using immunoelectron microscopy and immunohistochemistry. This study provides a time line for future studies to determine the molecular properties of lamprey cartilage development, and to correlate these properties with morphological events.

REFERENCES

ARMSTRONG LA, WRIGHT GM, YOUSON JH. Transformation of mucocartilage to a definite cartilage during metamorphosis in the sea lamprey, *Petromyzon marinus*. J Morphol 1987; 194: 1-21.

BENJAMIN M. The cranial cartilages of teleosts and their classification. J Anat 1990; 169: 153-172.

BRUCKNER P, VAN DER REST M. Structure and function of cartilage collagens. Microsc Res Tech 1994; 28: 378-384.

CARLSON BM. Patten's foundation of embryology. 5th ed. Toronto: McGraw-Hill Publishing Company, 1988.

COELHO CND, KOSHER RA. Gap junctional communication during limb cartilage differentiation. Dev Biol 1991; 144: 47-53.

CREMER MA, ROSLONIEC EF, KANG AH. The cartilage collagens: a review of their structure, organization, and role in the pathogenesis of experimental arthritis in animals and in human rheumatic disease. J Mol Med 1998; 76:275-288.

CUBBAGE CC, MABEE PM. Development of the cranium and paired fins in the zebrafish *Danio rerio* (*Ostariophysi, Cyprinidae*). J Morphol 1996; 229: 121-160.

DAMAS H. Recherches sur le développement de *Lampetra fluviatilis* L. Contribution à l'étude de la céphalogènese des Vertébrés. Arch Biol (Paris) 1944; 55: 1-284.

DEBEER G. The development of the vertebrate skull. Oxford: Clarendon Press, 1971.

DYKSTRA MJ. A Manual of Applied Techniques for Biological Electron Microscopy. New York: Plenum Press, 1993.

EDE DA. Cellular condensations and chondrogenesis. In: Hall, BK, ed. Cartilage, vol 2. Development, differentiation, and growth. Toronto: Academic Press, 1983: 143-185.

ERLEBACHER A, FILVAROFF EH, GITELMAN SE, DERYNCK R. Towards a molecular understanding of skeletal development. Cell 1995; 80: 371-378.

FAWCETT DW. A textbook of histology. 11th ed. Philadelphia: WB Saunders Company, 1986.

FOREY P, JANVIER P. Agnathans and the origin of jawed vertebrates. Nature 1993;

361: 129-134.

FRANZBLAU C, FARIS B. Elastin. In: Hay ED, ed. Cell biology of extracellular matrix. New York: Plenum Press, 1981: 65-94.

GILBERT SF. Developmental biology. Massachusetts: Sinauer Ass. Inc., 1997.

HALL BK, MIYAKE T. The membranous skeleton: The role of cell condensations in vertebrate skeletogenesis. Anat Embryol 1992; 186: 107-124.

HALL BK, MIYAKE T. Divide, accumulate, differentiate: cell condensation in skeletal development revisited. Int J Dev Biol 1995; 39: 881-893.

HARDISTY MW. Biology of the cyclostomes. London: Chapman and Hall, 1979.

HARDISTY MW. The skeleton. In: Hardisty MW, Potter IC, eds. The biology of lampreys. Vol 3. London: Academic Press, 1981: 333-376.

HARDISTY MW, POTTER IC. The general biology of adult lampreys. In: Hardisty MW, Potter IC, eds. The biology of lampreys, Vol 1. London: Academic press, 1971:127-206.

HILDEBRAND M. Analysis of vertebrate structure. Toronto: John Wiley and Sons, 1974.

HINCHLIFFE JR, JOHNSON DR. Growth of cartilage. In: Hall, BK, ed. Cartilage, Vol 2. Development, differentiation, and growth. Toronto: Academic Press, 1983: 255-296.

HUMASON GL. Animal Tissue Techniques, 4th ed. San Francisco: W.H. Freeman and Company, 1972.

HUYSSEUNE A, SIRE JY. Development of cartilage and bone tissues of the anterior part of the mandible in the cichlid fish: A light and TEM study. Anat Rec 1992; 233: 357-375.

JANVIER P. Patterns of diversity in the skull of jawless fishes. In: Hanken J and Hall BK, eds. The skull, vol 2. Patterns of structural and systemic diversity. Chicago: Chicago Press, 1993: 131-188.

JANVIER P. The dawn of the vertebrates: Characters versus common ascent in the rise of current vertebrate phylogenies. Paleontology 1996; 39: 259-287.

JOHNELS AG. On the development and morphology of the skeleton of the head of Petromyzon. Acta Zool (Stockh.) 1948; 29: 140-279.

JUNQUEIRA LC, CARNEIRO J, KELLEY RO. Basic histology, 9th ed. California: Lange Medical Pub., 1998.

KENT GC. Comparative anatomy of the vertebrates. 7th ed. Iowa: Wm. C. Brown Communications, 1987.

KIERNAN JA. Histological and histochemical methods: Theory and practice. 2nd ed. New York: Permagon Press, 1990.

KIMMEL CB, MILLER CT, KRUZE G, ULLMANN, BREMILLER RA, LARISON KD, SNYDER HC. The shaping of pharyngeal cartilages during early development of the zebrafish. Dev. Biol. 1998; 203: 245-263.

KOSHER RA. Chondroblast and chondrocyte. In: Hall BK, ed. Cartilage, vol 1. Structure, function and biochemistry. Toronto: Academic Press, 1983: 59-85.

KOSTOVIĆ-KNEŽEVIĆ L, BRADAMANTE Ž, ŠVAJGER A. On the ultrastructure of the developing elastic cartilage in the rat external ear. Anat Embryol 1986; 173: 385-391.

LANGILLE RM, HALL BK. Role of the neural crest in development of the trabeculae and branchial arches in the embryonic sea lamprey, *Petromyzon marinus L.* Development 1988; 102: 301-310.

LANGILLE RM, HALL BK. Pattern formation and the neural crest. In: Hanken J and Hall BK, eds. The skull, vol 1. Development. Chicago: Chicago Press, 1993: 77-111.

LØVTRUP S. The Phylogeny of the Vertebrata. New York: Wiley & Sons, 1977.

MAYNE R, von der MARK K. Collagens of cartilage. In: Hall BK, ed. Cartilage, vol 1. structure, function and biochemistry. Toronto: Academic Press, 1983: 181-214.

McBURNEY KM. Chondrogenesis and lamprin expression in developmental stages of the sea lamprey, *Petromyzon marinus*. M.Sc. Thesis, University of Prince Edward Island, Charlottetown: 1995.

McBURNEY KM, KEELEY FW, KIBENGE FSB, WRIGHT GM. Detection of lamprin mRNA in the anadromous sea lamprey using *in situ* hybridization. Biotech Histochem 1996a; 71: 44-53.

McBURNEY KM, KEELEY FW, KIBENGE FSB, WRIGHT GM. Spatial and temporal distribution of lamprin mRNA during chondrogenesis of trabecular cartilage in the sea lamprey. Anat Embryol 1996b; 193:419-426.

McBURNEY KM, WRIGHT GM. Chondrogenesis of a non-collagen-based cartilage in the sea lamprey, *Petromyzon marinus*. Can J Zool 1996; 74: 2118-2130.

MECHAM RP, HEUSER JE. Three-dimentional organization of extracellular matrix in elastic cartilage as viewed by quick freeze, deep etch electron microscopy. Connect Tiss Res 1990; 24: 83-93.

MECHAM RP. Elastin. In: Kreis T and Vale R, eds. Guidebook to the extracellular matrix and adhesion proteins. New York: Oxford University Press, 1993: 50-52.

MORGELIN M, PAULSSON M, HEINEGARD D, AEBI U, EHGEL J. Evidence of a defined spatial arrangement of hyaluronate in the central filament of cartilage proteoglycan aggregates. Biochem J 1995; 307: 595-601.

MONTES GS. Distribution of oxytalan, elaunin and elastic fibres in tissues. Ciencia e Cultura. 1992; 224-233.

MUIR H. The chondrocyte, architect of cartilage. Biomechanics, structure, function and molecular biology of cartilage matrix macromolecules. Bioessays 1995; 17: 1039-1048.

NEWTH DR. On the neural crest of lamprey embryos. J Embryol Exp Morph 1956; 4: 358-375.

PARKER WK. On the skeleton of Marsipobranch fishes. Phil Trans R Soc Lond 1883; 174: 411-458.

PASQUALI-RONCHETTI I, FOURNIERI C, BACCARANI-CONTRI M, QUAGLINO D. Ultrastructure of Elastin. In: The molecular biology and pathology of elastic tissues. CIBA Foundation Symposium192. Chichester: John Wiley and Sons, 1995: 31-50

PIAVIS GW. Embryological stages in the sea lamprey and effects of temperature on development. U.S. Fish Wildl Serv Bull 1961; 61: 111-143.

PIAVIS GW. Embryology. In: Hardisty MW, Potter IC, eds. The Biology of Lampreys, Vol 1. New York: Academic Press, 1971: 361-399.

ROBSON P, WRIGHT GM, SITARZ E, MAITI A, RAWAT M, YOUSON JH, KEELEY FW. Characterization of lamprin, an unusual matrix protein from lamprey cartilage. J Biol Chem 1993; 268: 1440-1447.

ROBSON P, WRIGHT GM, YOUSON JH, KEELEY FW. A family of non collagen-based cartilages in the skeleton of the sea lamprey, *Petromyzon marinus*. Comp Biochem Physiol 1997; 118B: 71-78.

SAGE H, GRAY WR. Studies on the evolution of elastin. I. Phylogenic distribution. Comp Biochem Physiol 1979; 68B: 473-480

SANDBERG MM. Matrix in cartilage and bone development: Current views on the function and regulation of major organic components. Ann Med 1991; 23:207-217.

SATO T. A modified method for lead staining of thin sections. J Electron Microsc 1968; 17: 158-159.

SERAFINI-FRACASSINI A. Elastogenesis in embryonic and post-natal development *In* Ruggeri A and Motta PM, eds. Ultrastructure of the connective tissue matrix. Boston: Martinus Nijoff Publishers, 1984: 140-149.

SHAFFER J. Die Stutzgewebe. In: Mollendorf WV, ed.. Handbuch der Mikroskopischen Anatomie des menschen, vol. 2. Berlin: Springer, 1930: 1-390.

SHELDON H. Transmission electron microscopy of cartilage. In: Hall BK, ed. Cartilage, vol 1. Structure, function and biochemistry. Toronto: Academic Press, 1983: 87-104.

SHILLING TF, KIMMEL CB. Musculoskeletal patterning in the pharyngeal segments of the zebrafish embryo. Development. 1997; 124: 2945-2960.

SHILLING TF, PIOTROWSKI T, HEINER G, BRAND M, HEISENBERG CP, JIANG YJ, BEUCHLE D, HAMMERSCHMIDT M, KANE DA, MULLINS MC, VAN EEDEN FJM, KELSH RN, FURUTANI-SEIKI M, GRANATO M, HAFFTER P, ODENTHAL J, WARGA RM, TROWE T, NIISSLEIN-VOLHARD C. Jaw and branchial arch mutants in zebrafish I: branchial arches. Development. 1996; 123: 329-344.

SMITH H. Evolution of chordate structure: An introduction to comparative anatomy. New York: Holt, Rinehart and Winston Inc., 1960.

SOLURSH M. Cell-cell interactions and chondrogenesis. In: Hall BK, ed. Cartilage, vol 2. Development, differentiation, and growth. Toronto: Academic Press, 1983: 121-142.

SOLURSH M., REITER RS. Evidence for histogenic interactions during *in vitro* limb chondrogenesis. Dev Biol 1980; 78: 141-150.

STOCKWELL RA. Biology of cartilage cells. New York: Cambridge University Press, 1979.

SWALLA BJ, UPHOLT WB, SOLURSH M. Analysis of type II collagen RNA localization in chick wing buds by *in situ* hybridization. Dev Biol 1988; 125: 51-58.

THOMAS JT, AYAD S, GRANT ME. Cartilage collagens: strategies for the organization and expression in the extracellular matrix. Ann Rheu Dis 1994; 53: 488-496.

THOROGOOD PV, HINCHLIFFE JR. An analysis of the condensation process during chondrogenesis in the embryonic chick hind limb. J Embryol Exp Morphol 1975; 33: 581-606.

VAN DER REST M, MAYNE R. Type IX collagen proteoglycan from cartilage is covalently cross-linked to type II collagen. J Biol Chem 1988; 263: 1615-1618.

VANDEWALLE P, FOCANT B, HURIAUX F, CHARDON M. Early development of the cephalic skeleton of *Barbus barbus* (*Teleostei, Cyprinidae*). J. Fish Biol. 1992; 41: 43-62.

WEBSTER D, WEBSTER M. Comparative vertebrate morphology. New York: Academic Press, 1974.

WEZEMAN FH. Morphological foundations of precartilage development in mesenchyme. Microsc Res Tech 1998; 43: 91-101.

WRIGHT GM, YOUSON JH. Ultrastructure of mucocartilage in the larval anadromous sea lamprey, *Petromyzon marinus* L. Am J Anat 1982; 165: 39-51.

WRIGHT GM, YOUSON JH. Ultrastructure of cartilage from young adult sea lamprey, *Petromyzon marinus* L: A new type of vertebrate cartilage. Am J Anat 1983; 167: 59-70.

WRIGHT GM, ARMSTRONG LA, JACQUES AM, YOUSON JH. Trabecular, nasal, branchial and pericardial cartilages in the sea lamprey, *Petromyzon marinus*: Fine structure and immunohistochemical detection of elastin. Am J Anat 1988; 182: 1-5.

WRIGHT GM, KEELEY FW, YOUSON JH. Lamprin: A new vertebrate protein comprising the major structural protein of adult lamprey cartilage. Experientia 1983; 39: 495-497.

WRIGHT GM, KEELEY FW, DEMONT ME Cartilage in the Atlantic hagfish *Myxine glutinosa*. In: Jørgensen M, Lomholt JP, Weber RE, Malte H eds. The biology of hagfishes. London: Chapman and Hall, 1998: 160-170.

YOUSON JH. Is lamprey metamorphosis regulated by thyroid hormones? Amer Zool 1997; 37:441-460.

6.1 APPENDIX A

Piavis staging criteria for *Petromyzon marinus*

Prolarval stage	Age (days pf)	Characteristics
14: Hatching	36811	yolk- filled gut, curved tail
15: Pigmentation	36906	tail straightens, heart enlarges, melanophores appear
16: Gill-cleft	15-17	mouth enlarges and becomes hooded, gill clefts appear and begin to function
17: Burrowing	17-33	prolarvae burrow into substrate, prominent eyespot, complete transparency, 9 -10 mm in length
18: Larval	33-40	all systems differentiated, can last from 3 to 17 years, grow to about 15 cm.

From: Piavis (1971)

6.2 APPENDIX B

Dehydration and infiltration of tissue for light microscopy:

70% ethanol	2 x 0.5 hour
95% ethanol	2 x 0.5 hour
100% ethanol	2 x 0.5 hour
50:50 100% ethanol: xylene	2 x 0.5 hour
xylene	2 x 0.5 hour
paraffin {Paraplast + Tissue embedding media (Fisher Scientific)}	2 x 0.5 hour

Place tissue in moulds filled with Paraplast + using an embedding center (Brinkman).

6.3 APPENDIX C

Dehydration and infiltration of tissue for electron microscopy:

Distilled water	1 x 10 minutes
50% ethanol	1 x 20 minutes
70% ethanol	2 x 10 minutes
95% ethanol	2 x 10 minutes
100% ethanol	2 x 15 minutes
Propylene Oxide	2 x 10 minutes
50:50 Epon: propylene oxide	30 minutes
75:25 Epon: propylene oxide	30 minutes
100% Epon	1 hour in vacuum desiccator

Put tissue in moulds, fill 2/3 with epon, place in vacuum desiccator overnight at 70°C